BNL-52526
UC-406

DYNAMICS OF SOLID-CONTAINING TANKS

A. S. Veletsos, A. H. Younan and K. Bandyopadhyay

January 1997

Prepared for
OFFICE OF ENVIRONMENTAL RESTORATION AND WASTE MANAGEMENT
DEPARTMENT OF ENERGY, WASHINGTON, D.C.

DISCLAIMER

ABSTRACT

Making use of a relatively simple, approximate but reliable method of analysis, a study is made of the responses to horizontal base shaking of vertical, circular cylindrical tanks that are filled with a uniform viscoelastic material. The method of analysis is described, and comprehensive numerical data are presented that elucidate the underlying response mechanisms and the effects and relative importance of the various parameters involved. In addition to the characteristics of the ground motion and a dimensionless measure of the tank wall flexibility relative to the contained medium, the parameters examined include the ratio of tank-height to tank-radius and the physical properties of the contained material. Both harmonic and earthquake-induced ground motions are considered. The response quantities investigated are the dynamic wall pressures, the critical forces in the tank wall, and the forces exerted on the foundation. Part A of the report deals with rigid tanks while the effects of tank wall flexibility are examined in Part B. A brief account is also given in the latter part of the interrelationship of the critical responses of solid-containing tanks and those induced in tanks storing a liquid of the same mass density.

TABLE OF CONTENTS

PART B. FLEXIBLE TANKS

LIST OF FIGURES

PART B. FLEXIBLE TANKS

LIST OF TABLES

EXECUTIVE SUMMARY

The study reported here is motivated by the need for improved understanding of the response to earthquakes of cylindrical tanks in nuclear facilities storing high-level radioactive wastes. The study complements those reported previously in Brookhaven National Laboratory reports 52378, 52417, 52420 and 52454.

In previous studies of this problem, the waste was modeled as a homogeneous or layered inviscid liquid. Although the mechanical properties of these wastes cannot accurately be defined at this time, their representation as ideal liquids may not generally be appropriate, and it is desirable to consider other idealizations.

In the present study, the waste is modeled as a uniform viscoelastic solid that is free at its upper surface and is bonded to a non-deformable base undergoing a uniform horizontal motion. The tank is presumed to be vertical and of circular cross section, and the interface of the tank wall and the contained material may be either smooth or rough. The objectives of the paper are: (1) To present a simple, approximate, yet reliable method of analysis for this system; and (2) through the study of comprehensive numerical solutions, to elucidate the underlying response mechanisms and the effects and relative importance of the various parameters involved. Part A of the report deals with rigid tanks, while Part B addresses the effects of wall flexibility on the assumption that the tank responds as a cantilever shear beam with no change in its cross section.

In addition to the characteristics of the ground motion, the parameters governing the response of the system are the ratio of tank-height to tank-radius, the physical properties of the contained material, and a dimensionless measure of the flexibility of the wall relative to that of the contained material. The response quantities examined are the dynamic wall pressures, the base shear and base moment in the wall, and the shear and moment exerted on the tank foundation. Both harmonic and earthquake-induced ground motions are considered. Special attention is paid to the effects of low-frequency, essentially static excitations. A maximum dynamic effect is then expressed as the product of the corresponding 'static' effect and an appropriate amplification or deamplification factor.

Following are the principal conclusions of the study:

1. For rigid, slender tanks with height-to-radius ratios H/R greater than about 3, the inertia forces for

all of the contained material are transmitted to the wall by horizontal extensional action, and practically the entire contained mass may be considered to be effective. With decreasing *H/R*, a progressively larger portion of the inertia forces gets transferred by horizontal shearing action to the base, and the portion of the retained mass that contributes to the wall forces is reduced significantly.

2. For a system of a specified *H/R*, the dynamic amplification factor depends importantly on the fundamental natural period of the contained material. This dependence is similar to, but by no means identical to, that obtained for a similarly excited, viscously damped single-degree-of-freedom oscillator. Specifically, for low-natural-period, stiff materials, the amplification factor is unity. With increasing flexibility or period of the contained material, the amplification factor increases and after attaining a nearly horizontal plateau, which for broad-banded earthquake ground motions may be of the order of 1.25 to 2.5, it decreases, reaching values less than unity. The larger amplification factors are attained for the slender tanks and for materials with low damping.

3. By decreasing the horizontal extensional stiffness of the retained material relative to its shearing stiffness, the flexibility of the wall reduces the proportion of the inertia forces transmitted to it by extensional action and increases the proportion transmitted to the base by horizontal shearing action. The flexibility of the wall also decreases the effective damping of the retained medium, and this reduction tends to increase the amplification factor of the dynamic response. With the exception of rather tall, slender systems with low to moderate wall flexibilities, for which both the shearing capacity and effective damping of the retained material are quite low, the net effect of wall flexibility is a reduction in peak response. This result is in sharp contrast with that obtained for liquid-containing tanks, for which the effect of wall flexibility is to increase rather that decrease the response.

4. For rigid tanks, the critical responses of solid-containing systems are generally substantially larger than those of liquid-containing systems of the same mass density, but for flexible tanks, particularly broad tanks of high wall flexibility, the opposite is likely to be true.

The comprehensive numerical data presented and the analysis of these data provide not only valuable insights into the effects and relative importance of the numerous parameters involved, but also a conceptual framework for the analysis and interpretation of the solutions for more involved systems as well.

ACKNOWLEDGMENT

This study was carried out at Rice University in cooperation with Brookhaven National Laboratory (BNL). The authors are grateful to the Department of Energy Program Directors and staff members John Tseng, James Antizzo, Dinesh Gupta, Kenneth Lang, David Pepson and Owen Thompson for supporting the study, and to Dr. Morris Reich of BNL for his understanding project management. Comments received from colleagues of BNL's Tank Seismic Experts Panel are also acknowledged with thanks.

PART A. RIGID TANKS

SECTION 1

INTRODUCTION

The study reported here is motivated by the need for improved understanding of the response to earthquakes of cylindrical tanks in nuclear facilities storing high-level radioactive wastes. The responses of these systems are normally evaluated on the assumption that the waste may be modeled as an incompressible, inviscid liquid. Although the mechanical properties of these wastes cannot accurately be defined at this time, their representation as ideal liquids may not generally be appropriate, and it is desirable to consider other idealizations.

In this paper, the waste is modeled as a uniform viscoelastic solid that is free at its upper surface and is bonded to a non-deformable base undergoing a uniform horizontal motion. The tank is presumed to be vertical, of circular cross section and rigid, and the interface of the tank wall and the contained material may be either smooth or rough. The objectives of the paper are: (a) To present a simple, approximate, yet reliable method of analysis for this system; and (b) through the study of comprehensive numerical solutions, to elucidate the underlying response mechanisms and the effects and relative importance of the various parameters involved. The effects of wall flexibility, which may be quite important for realistic tanks, are examined in Part B of the report.

In addition to the characteristics of the ground motion, the parameters governing the response of the system are the ratio of tank-height to tank-radius and the physical properties of the contained material. The response quantities examined are the dynamic wall pressures, the base shear and base moment in the wall, and the shear and moment exerted on the tank foundation. Both harmonic and earthquake-induced ground motions are considered. Special attention is paid to the effects of low-frequency, essentially static excitations. A maximum dynamic effect is then expressed as the product of the corresponding static effect and an appropriate amplification or deamplification factor.

The information presented is also applicable to the evaluation of the dynamic response of grain-storage tanks. As far as it can be determined, the most comprehensive study of the latter problem is the one reported by Rotter and Hull (1989). Although of great value, however, this study was limited to the static effects of the rigid-body inertia forces and did not provide for the true dynamic aspects of the problem.

SECTION 2

SYSTEM CONSIDERED

The system examined is shown in Fig. 2.1. It is a vertical, rigid, circular cylindrical tank of radius R that is filled to a height H with a homogeneous, linear viscoelastic solid. The tank is presumed to be fixed to a rigid base undergoing a space-invariant, uniform horizontal motion. The acceleration of the ground motion at any time t is denoted by $\ddot{x}_g(t)$ and its maximum value by $\ddot{X}_g$. The contained medium is considered to be free at its upper surface and bonded to its base. The interface conditions along the cylindrical boundary are identified later. Points on the tank or in the contained medium are defined by the cylindrical coordinate system, r, θ, z, the origin of which is taken at the center of the tank base, as shown in Fig. 2.1.

The properties of the medium are defined by its mass density ρ, shear modulus of elasticity G, Poisson's ratio ν, and the damping factor δ, which is considered to be frequency-independent and the same for both shearing and axial deformations. The latter factor is the same as the $\tan\delta$ factor used by the senior author and his associates in studies of foundation dynamics and soil-structure interaction (e.g., Veletsos and Verbic, 1973; Veletsos and Dotson, 1988), and twice as large as the percentage of critical damping used by other authors in related studies (e.g., Roesset et al. 1973; Pais and Kausel, 1988).

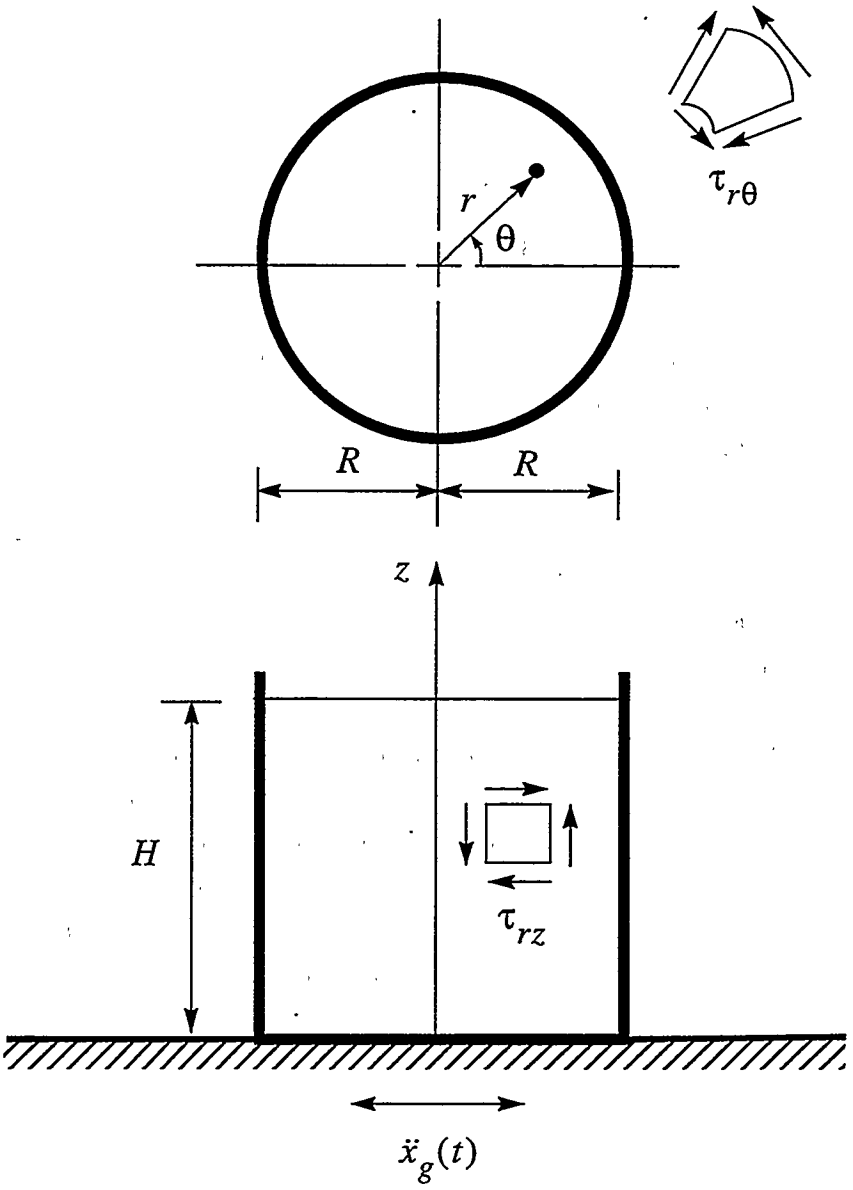

Fig. 2.1 System Considered

SECTION 3

METHOD OF ANALYSIS

3.1 Governing Equations and Assumptions

The method of analysis employed is similar to that used by Veletsos and Younan (1994a) for the evaluation of the dynamic soil pressures induced by horizontal base shaking on a cylinder embedded in a viscoelastic stratum. It assumes that, for the horizontal excitation considered, no vertical normal stresses develop anywhere in the medium, i.e. $\sigma_z = 0$. It further assumes that the horizontal variations of the vertical displacements are negligibly small, so that the radial and circumferential components of the shearing stresses on the top and bottom faces of an infinitesimal element, τ_{zr} and $\tau_{z\theta}$, may be expressed as

$$\tau_{zr} = \frac{G^*}{H}\frac{\partial u}{\partial \eta} \tag{1}$$

$$\tau_{z\theta} = \frac{G^*}{H}\frac{\partial v}{\partial \eta} \tag{2}$$

where u and v are the radial and circumferential components of the displacement relative to the moving base of an arbitrary point of the contained material defined by the dimensionless position coordinates $\xi = r/R$ and $\eta = z/H$, and G^* = the complex-valued shear modulus for the material. This modulus is related to the corresponding real-valued modulus G by

$$G^* = G(1 + i\delta) \tag{3}$$

where $i = \sqrt{-1}$. The radial and circumferential normal stress components σ_r and σ_θ, and the shearing stress component $\tau_{r\theta}$ are related to u and v by

$$\sigma_r = \psi_o^2\frac{G^*}{R}\frac{\partial u}{\partial \xi} + (\psi_o^2 - 2)\frac{G^*}{R}\left[\frac{1}{\xi}\frac{\partial v}{\partial \theta} + \frac{u}{\xi}\right] \tag{4}$$

$$\sigma_\theta = \psi_o^2\frac{G^*}{R}\left[\frac{1}{\xi}\frac{\partial v}{\partial \theta} + \frac{u}{\xi}\right] + (\psi_o^2 - 2)\frac{G^*}{R}\frac{\partial u}{\partial \xi} \tag{5}$$

$$\tau_{r\theta} = \frac{G^*}{R}\left[\frac{1}{\xi}\frac{\partial u}{\partial \theta} + \frac{\partial v}{\partial \xi} - \frac{v}{\xi}\right] \tag{6}$$

where

$$\psi_o = \sqrt{\frac{2}{1-\nu}} \tag{7}$$

The sign convention for stresses and displacements is that used in theory of elasticity. Specifically, displacements are positive when directed along the positive direction of the corresponding coordinate axis; normal stresses are positive when they induce tension; and the positive directions of the shearing stresses are as indicated in the inset diagrams of Fig. 2.1. The equations of motion for the medium in the radial and circumferential directions may then be expressed as

$$\psi_o^2 \frac{\partial}{\partial\xi}\left[\frac{1}{\xi}\frac{\partial}{\partial\xi}(\xi u) + \frac{1}{\xi}\frac{\partial v}{\partial\theta}\right] - \frac{1}{\xi}\frac{\partial}{\partial\theta}\left[\frac{1}{\xi}\frac{\partial}{\partial\xi}(\xi v) - \frac{1}{\xi}\frac{\partial u}{\partial\theta}\right] + \frac{R^2}{H^2}\frac{\partial^2 u}{\partial\eta^2} = \frac{\rho R^2}{G^*}\left[\frac{\partial^2 u}{\partial t^2} + \ddot{x}_g \cos\theta\right] \tag{8}$$

$$\psi_o^2 \frac{1}{\xi}\frac{\partial}{\partial\theta}\left[\frac{1}{\xi}\frac{\partial}{\partial\xi}(\xi u) + \frac{1}{\xi}\frac{\partial v}{\partial\theta}\right] + \frac{\partial}{\partial\xi}\left[\frac{1}{\xi}\frac{\partial}{\partial\xi}(\xi v) - \frac{1}{\xi}\frac{\partial u}{\partial\theta}\right] + \frac{R^2}{H^2}\frac{\partial^2 v}{\partial\eta^2} = \frac{\rho R^2}{G^*}\left[\frac{\partial^2 v}{\partial t^2} - \ddot{x}_g \sin\theta\right] \tag{9}$$

These equations differ from those reported in Veletsos and Younan (1994a) in that the factor ψ_o replaces the factor ψ_e, the difference stemming from the use of the simplified relations defined by (1) and (2).

Equations (8) and (9) are solved subject to the boundary conditions

$$u|_{\eta=0} = v|_{\eta=0} = 0 \tag{10}$$

$$\left.\frac{\partial u}{\partial\eta}\right|_{\eta=1} = \left.\frac{\partial v}{\partial\eta}\right|_{\eta=1} = 0 \tag{11}$$

of which the first set expresses the condition of complete bonding or rough interface between the medium and the base, and the second set expresses the vanishing of the horizontal shearing stresses at the upper surface. At the interface of the medium and the curved boundary, there is presumed to exist complete continuity in radial displacements, i.e.

$$u|_{\xi=1} = 0 \tag{12}$$

which, by virtue of the approximation involved in (1), also implies the absence of any vertical shearing stresses τ_{rz}. Two different interface conditions are considered for the circumferential motion in the horizontal plane: a rough interface, for which

$$v|_{\xi=1} = 0 \tag{13}$$

and a smooth interface, for which

$$\tau_{r\theta}\big|_{\xi=1} = 0 \tag{14}$$

It should be noted that the equilibrium of vertical forces is not satisfied in this approach. For long rectangular tanks (Veletsos *et al.*, 1995), and for straight walls retaining a semi-infinite layer (Veletsos and Younan, 1994b), it has been shown that this violation, as well as the other approximations referred to, do not affect materially the magnitudes of the wall pressures and forces which are the quantities of primary interest in this study. The same is expected to be true of the cylindrical system considered here.

3.2 Harmonic Response

For a harmonic base motion of acceleration

$$\ddot{x}_g(t) = \ddot{X}_g e^{i\omega t} \tag{15}$$

in which ω = its circular frequency, the resulting steady-state harmonic displacements u and v can be expressed as

$$u(\xi, \theta, \eta, t) = U(\xi, \eta)\cos\theta\, e^{i\omega t} \tag{16}$$

$$v(\xi, \theta, \eta, t) = V(\xi, \eta)\sin\theta\, e^{i\omega t} \tag{17}$$

where U and V are functions of the ξ and η coordinates. On expanding the unit functions associated with the ground acceleration terms on the right-hand members of (8) and (9) in the form

$$1 = \frac{4}{\pi}\sum_{n=1}^{\infty}\frac{1}{2n-1}\sin\left[\frac{(2n-1)\pi}{2}\eta\right] \tag{18}$$

the displacement amplitudes U and V may be expressed similarly as

$$U(\xi, \eta) = \sum_{n=1}^{\infty} U_n(\xi)\sin\left[\frac{(2n-1)\pi}{2}\eta\right] \tag{19}$$

$$V(\xi, \eta) = \sum_{n=1}^{\infty} V_n(\xi)\sin\left[\frac{(2n-1)\pi}{2}\eta\right] \tag{20}$$

where U_n and V_n are functions of the radial position coordinate ξ. It should be noted that the functions of η in (18), (19) and (20) represent the natural modes of vibration of the contained material when it is considered to act as an unconstrained, vertical, cantilever shear-beam, and that these functions satisfy the boundary conditions defined by (10) and (11).

On substituting (15) through (20) into (8) and (9), one obtains for each value of n a system of coupled

ordinary differential equations in U_n and V_n. These equations may be decoupled by expressing U_n and V_n in terms of the potential functions P_n and S_n used by Tajimi (1973) as

$$U_n = \frac{dP_n}{d\xi} + \frac{S_n}{\xi} \tag{21}$$

$$V_n = -\frac{P_n}{\xi} - \frac{dS_n}{d\xi} \tag{22}$$

The solution of the resulting ordinary differential equations in P_n and S_n may then be expressed as

$$P_n(\xi) = A'_n I_1(\alpha_n \xi) + C'_n K_1(\alpha_n \xi) + \frac{1}{2}\xi U_n^f \tag{23}$$

$$S_n(\xi) = B'_n I_1(\beta_n \xi) + D'_n K_1(\beta_n \xi) + \frac{1}{2}\xi U_n^f \tag{24}$$

in which I_1 and K_1 are modified Bessel functions of the first order and first and second kind, respectively; A'_n through D'_n are integration constants that remain to be determined; α_n and β_n are dimensionless factors given by

$$\alpha_n = \frac{\beta_n}{\psi_o} \tag{25}$$

$$\beta_n = \frac{(2n-1)\pi}{2}\frac{R}{H}\sqrt{1 - \frac{\phi_n^2}{1+i\delta}} \tag{26}$$

with

$$\phi_n = \frac{\omega}{\omega_n} \tag{27}$$

$$\omega_n = \frac{(2n-1)\pi}{2}\frac{v_s}{H} \tag{28}$$

and $v_s = \sqrt{G/\rho}$ = the shear wave velocity for the medium; and

$$U_n^f = -\frac{16\rho \ddot{X}_g H^2}{\pi^3 G}\frac{1}{(2n-1)^3}\frac{1}{1-\phi_n^2+i\delta} \tag{29}$$

It should be noted that ω_n represents the *n*th circular natural frequency of the contained material when it is considered to act as an unconstrained, cantilever shear-beam, and that U_n^f represents the maximum displacement amplitude of the shear-beam to the specified base motion. The superscript *f* in the latter symbol is used to emphasize the fact that the shear-beam displacement defines the far-field action of the stratum. Additional details of the method of analysis may be found in Veletsos and Younan (1994a).

On deleting from (23) and (24) the terms with the function K_1 which increase without bound as

$\xi \to 0$, and substituting the expressions for P_n and S_n into (21) and (22), one obtains

$$U_n = \left\{1 - A_n\left[\alpha_n I_0(\alpha_n\xi) - \frac{1}{\xi} I_1(\alpha_n\xi)\right] - B_n \frac{1}{\xi} I_1(\beta_n\xi)\right\} U_n^f \tag{30}$$

$$V_n = -\left\{1 - A_n \frac{1}{\xi} I_1(\alpha_n\xi) - B_n\left[\beta_n I_0(\beta_n\xi) - \frac{1}{\xi} I_1(\beta_n\xi)\right]\right\} U_n^f \tag{31}$$

where I_0 = the modified Bessel function of the first kind and zero order; and the constants A_n and B_n are related to A_n' and B_n' by

$$\frac{A_n'}{A_n} = \frac{B_n'}{B_n} = -U_n^f \tag{32}$$

The integration constants A_n and B_n may now be determined by satisfying the boundary conditions defined by (12) and either (13) or (14). For the rough interface defined by (12) and (13),

$$A_n = \frac{1}{\Delta_n}\left[\beta_n I_0(\beta_n) - 2 I_1(\beta_n)\right] \tag{33a}$$

$$B_n = \frac{1}{\Delta_n}\left[\alpha_n I_0(\alpha_n) - 2 I_1(\alpha_n)\right] \tag{33b}$$

and

$$\Delta_n = \alpha_n I_0(\alpha_n)\left[\beta_n I_0(\beta_n) - I_1(\beta_n)\right] - \beta_n I_0(\beta_n) I_1(\alpha_n) \tag{33c}$$

whereas for the smooth interface defined by (12) and (14),

$$A_n = \frac{1}{\Delta_n}\left[2\beta_n I_0(\beta_n) - (4 + \beta_n^2) I_1(\beta_n)\right] \tag{34a}$$

$$B_n = \frac{1}{\Delta_n}\left[2\alpha_n I_0(\alpha_n) - 4 I_1(\alpha_n)\right] \tag{34b}$$

and

$$\Delta_n = \left[\alpha_n I_0(\alpha_n) - I_1(\alpha_n)\right]\left[2\beta_n I_0(\beta_n) - \beta_n^2 I_1(\beta_n)\right] - 2\alpha_n I_0(\alpha_n) I_1(\beta_n) \tag{34c}$$

Dynamic Wall Pressures and Shearing Stresses

The dynamic components of the radial or normal pressures, σ_r, and of the circumferential shearing stresses, $\tau_{r\theta}$, induced on the medium-wall interface may be expressed in forms analogous to (16) and (17) as

$$\sigma_r = \sigma(\eta)\cos\theta\, e^{i\omega t} \tag{35}$$

$$\tau_{r\theta} = \tau(\eta)\sin\theta\, e^{i\omega t} \tag{36}$$

where $\sigma(\eta)$ and $\tau(\eta)$ are complex-valued amplitudes that are functions of the η coordinate. On substituting (35) and (36) into (4) and (6), making use of (15) through (20) and (30) and (31), it is found that

$$\sigma(\eta) = -\frac{8\psi_o}{\pi^2}\rho\ddot{X}_g H \sum_{n=1}^{\infty} \frac{g_n}{(2n-1)^2}\sqrt{\frac{1+i\delta}{1-\phi_n^2+i\delta}}\sin\left[\frac{(2n-1)\pi}{2}\eta\right] \tag{37}$$

and

$$\tau(\eta) = \frac{8}{\pi^2}\rho\ddot{X}_g H \sum_{n=1}^{\infty} \frac{h_n}{(2n-1)^2}\sqrt{\frac{1+i\delta}{1-\phi_n^2+i\delta}}\sin\left[\frac{(2n-1)\pi}{2}\eta\right] \tag{38}$$

where g_n and h_n are dimensionless factors which, for a rough interface, are given by

$$g_n = \frac{1}{\Delta_n}\alpha_n I_1(\alpha_n)\left[2I_1(\beta_n) - \beta_n I_0(\beta_n)\right] \tag{39a}$$

and

$$h_n = \frac{1}{\Delta_n}\beta_n I_1(\beta_n)\left[2I_1(\alpha_n) - \alpha_n I_0(\alpha_n)\right] \tag{39b}$$

and for a smooth interface, they are given by

$$g_n = \frac{\alpha_n}{\Delta_n}\left\{\left[(4+\beta_n^2)I_1(\beta_n) - 2\beta_n I_0(\beta_n)\right]I_1(\alpha_n) - \left[\alpha_n I_0(\alpha_n) - 2I_1(\alpha_n)\right]2I_1(\beta_n)\right\} \tag{40a}$$

and

$$h_n = 0 \tag{40b}$$

Base Shear and Base Moment

With the stress amplitudes along the wall-solid interface established, the amplitudes of the base shear Q_b and of the overturning base moment M_b induced by these stresses are determined by integration to be

$$\begin{aligned} Q_b &= \int_0^1\int_0^{2\pi}[\tau(\eta)\sin^2\theta - \sigma(\eta)\cos^2\theta]R\,d\theta H\,d\eta \\ &= -m\ddot{X}_g \frac{16}{\pi^3}\frac{H}{R}\sum_{n=1}^{\infty}\frac{\psi_o g_n + h_n}{(2n-1)^3}\sqrt{\frac{1+i\delta}{1-\phi_n^2+i\delta}} \end{aligned} \tag{41}$$

and

$$M_b = \int_0^1 \int_0^{2\pi} [\tau(\eta)\sin^2\theta - \sigma(\eta)\cos^2\theta] R d\theta \, H^2 \eta \, d\eta$$
$$= -m\ddot{X}_g H \frac{32}{\pi^4} \frac{H}{R} \sum_{n=1}^{\infty} \frac{(-1)^{n-1}}{(2n-1)^4} (\psi_o g_n + h_n) \sqrt{\frac{1+i\delta}{1-\phi_n^2+i\delta}} \quad (42)$$

where $m = \pi \rho R^2 H$ = the total mass of the contained solid.

3.3 Transient Response

The response of the system to an arbitrary transient excitation is evaluated from the harmonic response by the Discrete Fourier Transform (DFT) approach in combination with the Fast Fourier Transform (FFT) algorithm. In the application of this procedure, the duration of the forcing function should be increased by the addition of a sufficiently long band of zeros to eliminate the aliasing errors that may be introduced. For the solutions presented here, the duration of the band was taken equal to either the duration of the forcing function or 10 times the fundamental natural period of the system considered, whichever was larger.

SECTION 4

WALL PRESSURES AND FORCES

It is desirable to begin by examining the responses obtained for excitations the dominant frequencies of which are small compared to the fundamental natural frequency of the stratum (i.e. for values of $\phi_1 \rightarrow 0$). Such excitations and the resulting effects will be referred to as **static**, a term which should not be confused with that normally used to represent the effects of gravity forces. The static effects are identified with the subscript *st*. The maximum value of a dynamic effect is then expressed as the product of the corresponding static effect and an appropriate amplification or deamplification factor.

4.1 Static Effects

As indicated by (35) and (36), the circumferential variation of the normal wall pressures induced by either static or dynamic excitations is proportional to $\cos\theta$, whereas that of the circumferential shearing stresses is proportional to $\sin\theta$. Accordingly, the maximum numerical values of the normal pressures occur at $\theta = 0$ and $180°$, and those of the shearing stresses occur at $\theta = 90°$ and $270°$.

The heightwise variations of the static normal pressures and of the circumferential shearing stresses exerted on the wall are shown in Fig. 4.1 normalized with respect to the maximum or top values. Systems with both smooth and rough interfaces and several different values of the slenderness ratio H/R are considered, with Poisson's ratio for the contained material taken as $\nu = 1/3$. The same value of ν is used for all other solutions presented here.

It is observed that for the relatively broad, stubby systems with low values of H/R, the stress distributions increase from the base to the top approximately as a quarter-sine curve whereas for the taller, more slender systems, the distribution is practically uniform.

The normalizing or top values of the stress amplitudes for systems with different slenderness ratios H/R are listed in Table 4.1, and they are also plotted in Fig. 4.2. These values are normalized with respect to $\rho\ddot{X}_g R$, the maximum normal wall pressure computed on the assumption that the medium-wall interface is smooth and that the full inertia of the contained material per unit of tank height is transferred horizontally to the wall. Therefore, in comparing the stress values in tanks of different proportions, the tank radii rather than the medium heights must be considered to be the same.

Increasing the slenderness ratio H/R increases the horizontal extensional stiffness of the contained medium relative to its shearing stiffness, and this increases the capacity of the medium to transfer the inertia forces horizontally to the wall. For the smooth interface, the normalized value of the normal pressure increases from zero for $H/R \rightarrow 0$ to unity for $H/R \rightarrow \infty$, whereas for the rough interface, it increases to a value of about 0.75, the difference between unity and 0.75 representing the normalized value of the shearing stress amplitude. Being the stiffer of the two, the rough interface attracts a higher proportion of the inertia forces than the smooth interface. However, because the rough interface resists these forces by a combination of normal pressures and circumferential shearing stresses while the smooth interface resists them entirely by normal pressures, the normal stresses for the rough interface are actually lower than for the smooth.

That the total wall force or base shear for the rough interface is indeed greater than for the smooth can clearly be seen in Fig. 4.3, which compares the results obtained over a wide range of the slenderness ratio H/R. The forces in this case are normalized with respect to $m\ddot{X}_g$, the total inertia of the contained medium when it is presumed to act as a rigid body. As would be expected, the effective or participating fraction of the contained mass increases with increasing H/R, reaching the full mass for the very tall, slender tanks. The normalized values of the base shear $(Q_b)_{st}$ and of the components $(Q_b^{\sigma})_{st}$ and $(Q_b^{\tau})_{st}$ contributed by the normal pressures and circumferential shearing stresses, respectively, are also listed in Table 4.1.

The static value of the overturning base moment induced by the wall pressures, $(M_b)_{st}$, may conveniently be expressed as the product of the base shear and an appropriate height *h*. The latter quantity, normalized with respect to the tank height *H*, is shown in Fig. 4.3 and is also listed in Table 4.1. For broad systems with low values of H/R, for which the vertical distributions of the interfacial wall stresses are approximately a quarter-sine, $h/H = 0.599$, a value close to the $2/\pi$ value obtained for the sinusoidal variation. As H/R increases, h/H decreases, reaching the limiting value of 0.5 corresponding to a uniform distribution.

Effects for Very Broad Systems

For very broad systems with values of $H/R \rightarrow 0$, it is more instructive to express the interfacial stresses in terms of $\rho\ddot{X}_g H$ rather than in terms of $\rho\ddot{X}_g R$. The maximum normal wall pressure at the top then reduces to

$$\sigma_{st}(1) = 0.741\psi_o\rho\ddot{X}_g H = 1.406\rho\ddot{X}_g H \tag{43}$$

and the corresponding circumferential shearing stress reduces to

$$\tau_{st}(1) = 0.741\rho\ddot{X}_g H \tag{44}$$

Similarly, the base shear may more conveniently be expressed in terms of $(\pi RH^2)\,\rho\ddot{X}_g$ rather than $m\ddot{X}_g = (\pi R^2 H)\,\rho\ddot{X}_g$. The values for a rough and a smooth interface are then

$$(Q_b)_{st} = 1.571\pi\rho\ddot{X}_g RH^2 \tag{45}$$

and

$$(Q_b)_{st} = 1.029\pi\rho\ddot{X}_g RH^2 \tag{46}$$

respectively. The pressure defined by (43) is identical to that reported in Veletsos and Younan (1994b) for the limiting case of a straight, rigid wall retaining a semi-infinite, uniform soil stratum.

4.2 Harmonic Effects

The steady-state amplitude of the total wall force or base shear in the wall of harmonically excited systems, $(Q_b)_{max}$, is plotted in Fig. 4.4 as a function of the frequency ratio ω/ω_1, where ω_1 = the fundamental circular frequency of the contained material when it is considered to respond as a cantilever shear-beam. Systems with values of H/R in the range between 0.3 and 3 are considered. The tank in these solutions is presumed to be massless; the interface between the tank wall and the contained material is considered to be rough; and Poisson's ratio and the damping factor for the contained material are taken as 1/3 and 0.1, respectively. As before, the results are normalized with respect to $m\ddot{X}_g$.

As would be expected, the curves are undulatory in nature, the peaks corresponding to the natural frequencies of the system. For broad systems with values of H/R of the order of 0.3 or less, the highest resonant peak is attained at a frequency $\omega \approx \omega_1$, and the associated amplification factor (defined as the ratio of the dynamic to the corresponding static responses) is relatively small. By contrast, for the more slender systems with the higher values of H/R, both the frequencies and the amplification factors of the fundamental resonant peaks are significantly higher, the larger amplification factors reflecting a reduced damping capacity for these systems. As the tank radius *R* is decreased, the waves in the medium must travel progressively shorter distances before they get reflected by the rigid boundary; accordingly, they are not affected as much by material damping as would be the case for the broader systems with the larger radii. As $H/R \to 0$, the amplification factor tends approximately to $1/\sqrt{\delta}$, a fact noted previously (Arias *et al.* 1981; Veletsos and Younan 1994b), and as $H/R \to \infty$, it tends to the value applicable to a long, rigid cylinder containing a viscoelastic solid. For the value of $\delta = 0.1$ considered here, these limiting values are 3.16 and 6.61, respectively.

Within the framework of the approximations involved in the method of analysis considered, the radial and circumferential displacements of the medium for the *m*th radial and the *n*th vertical natural mode of vibration may be expressed as

$$u(\xi, \theta, \eta, t) = \mathcal{U}_m(\xi) \sin\left[\frac{(2n-1)\pi}{2}\eta\right] \cos\theta \; e^{i\omega_{mn}t} \tag{47}$$

$$v(\xi, \theta, \eta, t) = \mathcal{V}_m(\xi) \sin\left[\frac{(2n-1)\pi}{2}\eta\right] \sin\theta \, e^{i\omega_{mn}t} \tag{48}$$

where ω_{mn} is the associated circular frequency, and $\mathcal{U}_m(\xi)$ and $\mathcal{V}_m(\xi)$ are functions of the dimensional coordinate ξ, the detailed expressions for which are given in the Appendix. The frequency ω_{mn} may be expressed in the form

$$\omega_{mn} = \sqrt{(2n-1)^2 + \left[\frac{2}{\pi}\frac{\Psi_o \gamma_m H}{R}\right]^2}\,\omega_1 \tag{49}$$

where γ_m = a dimensionless factor which, in addition to the order of the horizontal mode of vibration, depends on Poisson's ratio of the material ν and the condition at the medium-wall interface; and ω_1, as already noted, refers to the fundamental circular frequency of the contained material when it is considered to respond as an unconstrained cantilever shear-beam. The first five values of γ_m for systems with $\nu = 1/3$ and either a rough or a smooth interface are listed in Table 4.2. As an illustration, it is noted that for a system with $H/R = 1$ and a rough interface, the first four values of ω_{m1}/ω_1 are 2.35, 3.57, 5.49 and 5.99. The first, second and fourth of these values practically coincide with the abscissas of the peaks of the relevant frequency response curve in Fig. 4.4. This fact, along the absence of any other peaks in the curve considered, indicate that the response of the system is dominated by the natural modes corresponding to the fundamental vertical mode and to several horizontal modes.

The validity of the latter statement can more clearly be seen in Fig. 4.5, in which the frequency response curves for the base shear in the tank wall presented previously in Fig. 4.4 using a sufficiently large number of terms are compared with those computed considering the contribution of the first term only. For improved clarity, the frequency scales in this case are normalized with respect to the fundamental circular frequency of the system under consideration, ω_{11}, rather than the corresponding frequency ω_1 of the unconstrained medium. The excellent agreement between the two solution sets suggests that the use of only the first term in the series should yield highly accurate results for broad-banded, transient ground motions as well.

Peak Amplification Factor

The variation with H/R of the largest amplification factor for base shear in the tank wall is shown in Fig. 4.6 for systems with material damping factors in the range between $\delta = 0.05$ and 0.20. Poisson's ratio for the material is taken as 1/3, and both rough and smooth interface conditions are examined. As previously indicated, the effective damping of systems with a specified δ decreases with increasing H/R, and this reduction leads to a corresponding increase in the amplification factor.

It is worth noting that the amplification factors for systems with the smooth interface are, with minor exceptions, lower than those for the rough interface. This unexpected result is attributed to the fact

that, whereas for the rough interface, the response of the system is dominated by the contribution of the fundamental mode of vibration, for the smooth interface, the contribution of the second horizontal mode is almost as important as that of the first. The inertia forces for these two modes of vibration of a system with $H/R = 1$ are shown in Fig. 4.7.

4.3 Seismic Effects

The solid lines in Fig. 4.8(a) define the maximum values of the base shear in the wall of systems subjected to the N-S component of the 1940 El Centro, California earthquake ground motion record. The acceleration, velocity and displacement traces of this record are available in Veletsos and Tang (1990) and are not reproduced here. The maximum value of the ground acceleration is $\ddot{X}_g = 0.312\,g$, where g = the gravitational acceleration, and the corresponding values of the velocity and displacement are $\dot{X}_g = 35.61$ cm/sec (14.02 in/sec) and $X_g = 21.05$ cm (8.29 in). As before, the tank in these solutions is presumed to be massless, the tank-medium interface is presumed to be rough, and Poisson's ratio and the damping factor of the retained material are taken as $\nu = 1/3$ and $\delta = 0.1$. The results are plotted as a function of the fundamental period of the system, $T_{11} = 2\pi\omega_{11}$, where ω_{11} is defined by (49), and they are normalized with respect to $m\ddot{X}_g$, the maximum value of the total inertia of the contained material when the latter is considered to act as a rigid body. The same information expressed as amplification factors (i.e., normalized with respect to the low-natural-period or static response of the system under consideration) is displayed in Fig. 4.8(b).

As an indication of the range of T_{11} values that may be encountered in practice, it is noted that for materials having shear-wave velocities in the range of 60 to 480 m/sec (197 and 1570 ft/sec) and tank heights in the range of 6 to 15 m (20 to 49 ft), the fundamental period of the material idealized as an unconstrained cantilever shear beam would be in the range of 0.05 to 1 sec. Depending on the slenderness of the tank, H/R, the fundamental period of the system would then fall in the following ranges:

- For $H/R = 0.3$, $T_{11} \cong 0.04$ to 0.84 sec.
- For $H/R = 0.5$, $T_{11} \cong 0.03$ to 0.68 sec.
- For $H/R = 1$, $T_{11} \cong 0.02$ to 0.42 sec.
- For $H/R = 3$, $T_{11} \cong 0.01$ to 0.15 sec.

The boundaries of these ranges are identified in Fig. 4.8(a) with dots.

The plots in Fig. 4.8 are similar to, but by no means the same as, the response spectra for similarly excited, viscously damped single-degree-of-freedom systems. Specifically, for low-natural-period, stiff materials, the maximum values of the dynamic base shear in the tank wall are equal to the static values listed in Table 4.1, and the amplification factors are unity. With increasing flexibility of the contained material, i.e., increasing natural period of the system, the dynamic effects increase, and

after attaining nearly horizontal plateaus, they decrease to values that may be substantially lower than the static effects. As already indicated, increasing H/R decreases the damping capacity of the system and increases the dynamic amplification factor.

Considering that the fundamental period of many practical, broad systems with values of $H/R \leq 1$ falls in the highly amplified region of the plots presented in Fig. 4.8, it is of special interest to examine the largest values of the amplification factors. The variation with H/R of the absolute maximum amplification factor for base shear in the tank wall is shown in Fig. 4.9 for systems with three different values of the damping factor δ. The solid lines are for systems with a rough medium-wall interface, whereas the dashed lines are for a smooth interface. Also shown in Fig. 4.9 are the average values of the amplification factors over the range of natural periods from 0.1 to 0.5 sec. As would be expected, these factors are significantly smaller than those for the maximum resonant peak of the harmonically excited systems considered in Fig. 4.6. Additionally, the results for the earthquake ground motion are substantially less sensitive to variations in the slenderness ratio H/R than are those for the harmonic excitation.

Overturning Base Wall Moment

Following the approach used for statically excited systems, the maximum value of the overturning base moment induced by the wall pressures may be expressed as the product of the maximum total wall force or base shear $(Q_b)_{max}$ and an appropriate height *h*. Normalized values of *h* for systems with a rough interface subjected to the El Centro ground motion record are plotted in Fig. 4.10 as a function of the fundamental period of the contained material T_{11}. It is observed that the results are insensitive to variations in T_{11} and may, therefore, be taken equal to those reported earlier for the low-natural-period, statically excited systems.

Relative Effects of Normal and Shearing Stresses

The base shear in the tank wall of systems with a rough interface is contributed partly by normal pressures and partly by circumferential shearing stresses. For the systems excited by the El Centro record, the component of the maximum base shear contributed by the normal pressures, $(Q_b^{\sigma})_{max}$, is plotted in Fig. 4.11 as a fraction of the corresponding total shear, $(Q_b)_{max}$. A range of natural periods T_{11} and three different values of the slenderness ratio H/R are considered. It is observed that the ratio varies from about 64% for very broad tanks with values of $H/R \rightarrow 0$ to about 90% for relatively slender tanks with values of $H/R = 3$.

Table 4.1: Static Values of Top Stresses, Base Whears and Effective Heights for Systems with Different Slenderness Ratios and Interface Conditions; $\nu = 1/3$

$\frac{H}{R}$	Rough Interface						Smooth Interface		
	$\frac{\sigma_{st}(1)}{\rho\ddot{X}_g R}$	$\frac{\tau_{st}(1)}{\rho\ddot{X}_g R}$	$-\frac{(Q_b^{\sigma})_{st}}{m\ddot{X}_g}$	$-\frac{(Q_b^{\tau})_{st}}{m\ddot{X}_g}$	$-\frac{(Q_b)_{st}}{m\ddot{X}_g}$	$\frac{h}{H}$	$\frac{\sigma_{st}(1)}{\rho\ddot{X}_g R}$	$-\frac{(Q_b)_{st}}{m\ddot{X}_g}$	$\frac{h}{H}$
(1)	(2)	(3)	(4)	(5)	(6)	(7)	(8)	(9)	(10)
0.00	$1.406\frac{H}{R}$	$0.741\frac{H}{R}$	$1.029\frac{H}{R}$	$0.542\frac{H}{R}$	$1.571\frac{H}{R}$	0.599	$1.406\frac{H}{R}$	$1.029\frac{H}{R}$	0.599
0.30	0.365	0.162	0.269	0.122	0.391	0.595	0.377	0.276	0.598
0.40	0.463	0.190	0.343	0.146	0.489	0.593	0.492	0.361	0.598
0.50	0.540	0.209	0.404	0.163	0.567	0.590	0.593	0.438	0.597
0.60	0.598	0.222	0.452	0.176	0.628	0.587	0.677	0.503	0.595
0.70	0.640	0.230	0.491	0.186	0.677	0.583	0.745	0.559	0.593
0.80	0.671	0.236	0.521	0.194	0.715	0.580	0.800	0.605	0.591
0.90	0.693	0.240	0.545	0.200	0.745	0.576	0.842	0.644	0.588
1.00	0.709	0.243	0.565	0.205	0.770	0.573	0.876	0.677	0.585
1.25	0.731	0.246	0.602	0.214	0.816	0.565	0.931	0.738	0.579
1.50	0.740	0.247	0.626	0.220	0.846	0.559	0.962	0.781	0.573
1.75	0.744	0.248	0.644	0.224	0.868	0.553	0.977	0.812	0.567
2.00	0.746	0.248	0.657	0.227	0.884	0.548	0.986	0.835	0.562
2.50	0.745	0.247	0.675	0.231	0.906	0.540	0.993	0.868	0.553
3.00	0.744	0.246	0.687	0.234	0.921	0.535	0.993	0.889	0.547
5.00	0.740	0.245	0.710	0.240	0.950	0.524	0.990	0.932	0.531
10.00	0.740	0.240	0.726	0.243	0.969	0.515	0.980	0.962	0.519

Table 4.2: Values of Factors γ_m, $\mathcal{A}_m$ and $\mathcal{B}_m$ in Expressions for Natural Frequencies and Vibration Modes of Contained Material; $\nu = 1/3$.

m	Rough Interface			Smooth Interface		
	γ_m	$\mathcal{A}_m$	$\mathcal{B}_m$	γ_m	$\mathcal{A}_m$	$\mathcal{B}_m$
(1)	(2)	(3)	(4)	(5)	(6)	(7)
1	1.9427	0.5991	0.2845	1.3150	13.9875	-7.1976
2	3.1056	0.1271	-0.4452	2.0125	0.3696	0.3604
3	4.8982	0.0737	0.1932	3.8796	0.0178	-0.3079
4	5.3559	0.5920	-0.1262	5.3259	0.3479	0.0159
5	6.7603	0.0183	0.1602	5.7592	0.0134	-0.2082

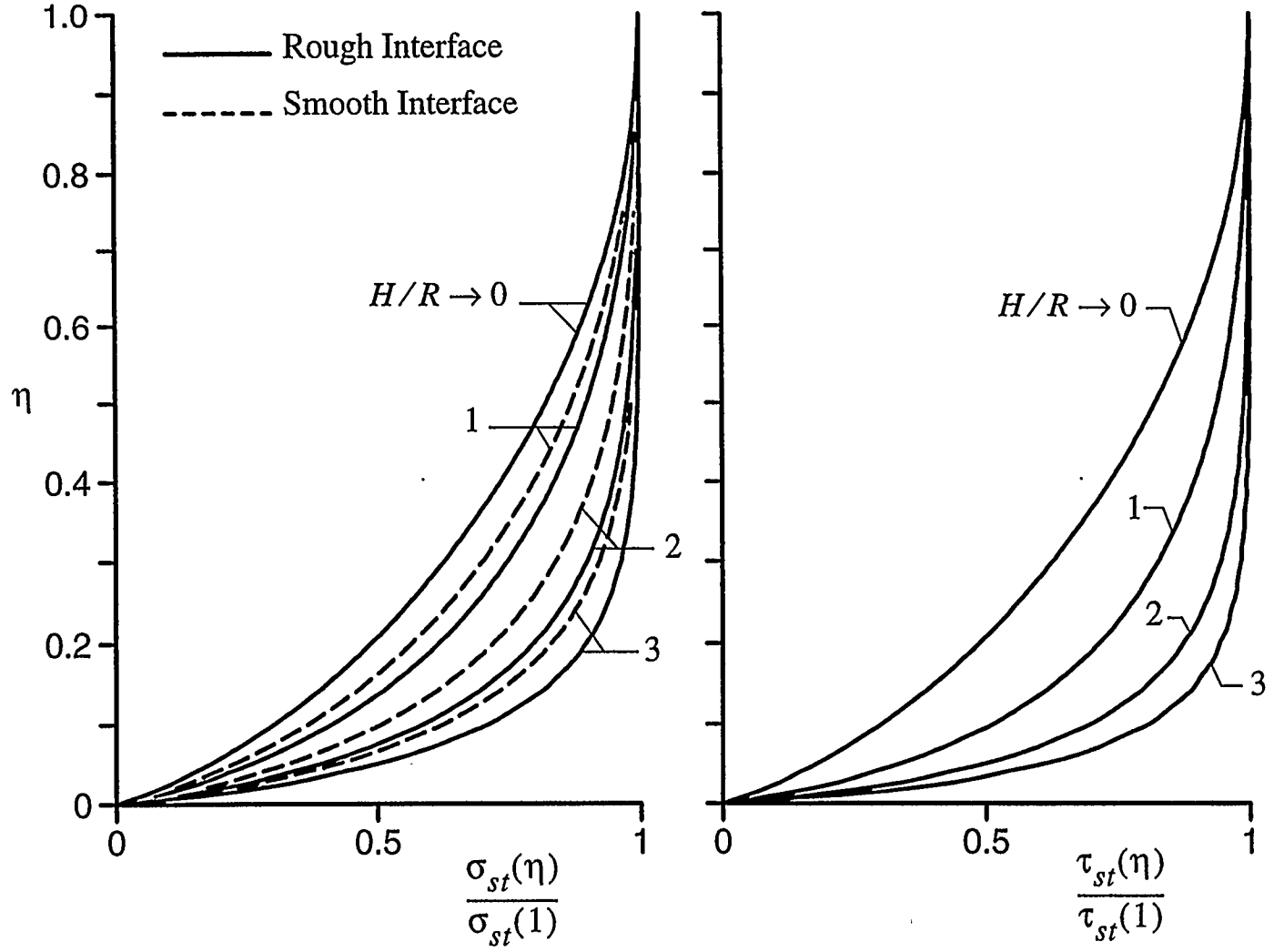

Fig. 4.1 Heightwise Variations of 'Static' Values of Normal and Circumferential Stresses Induced on Tanks with Different Aspect Ratios; $\nu = 1/3$.

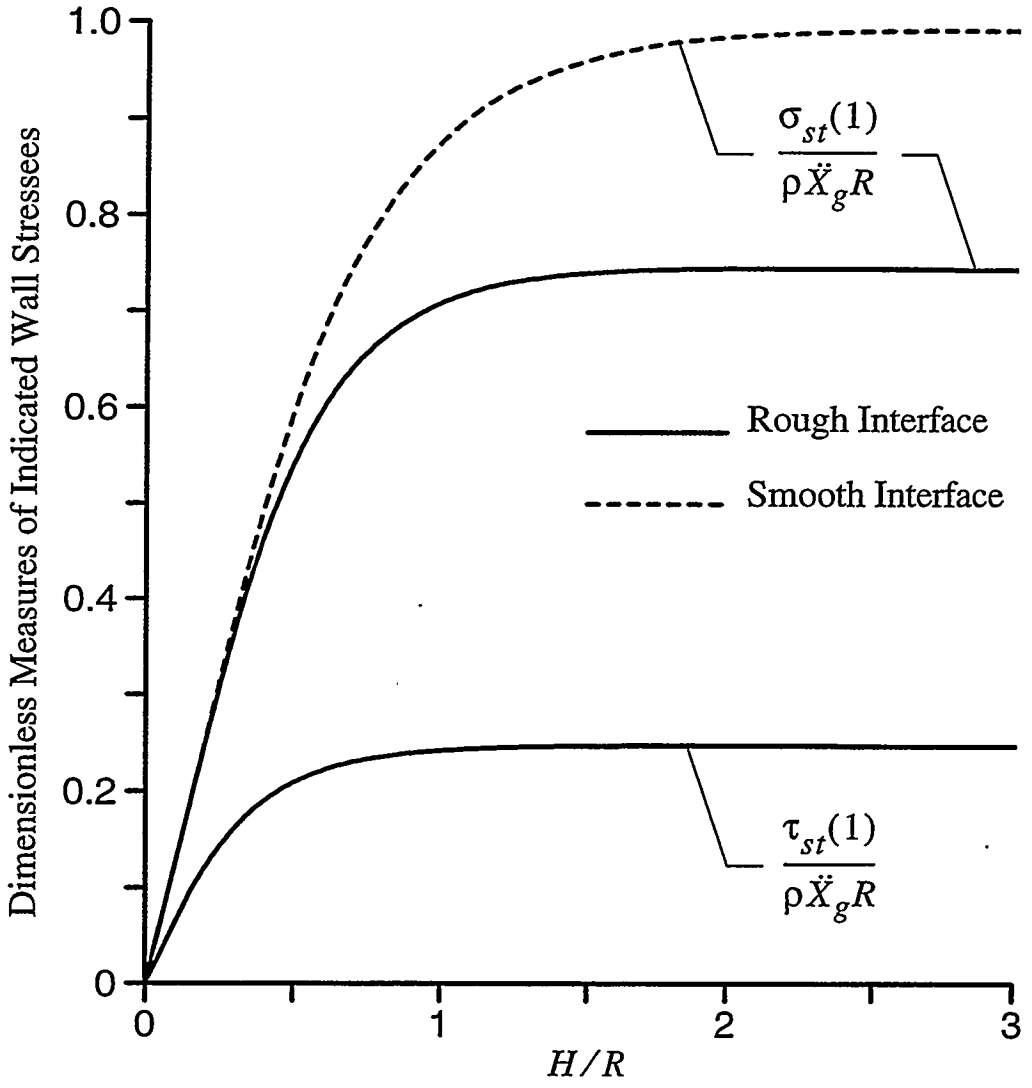

Fig. 4.2 Effect of Slenderness Ratio, H/R, on Maximum Static Values of Normal Pressure and of Circumferential Shearing Stress Induced at Top of Tank; $\nu = 1/3$.

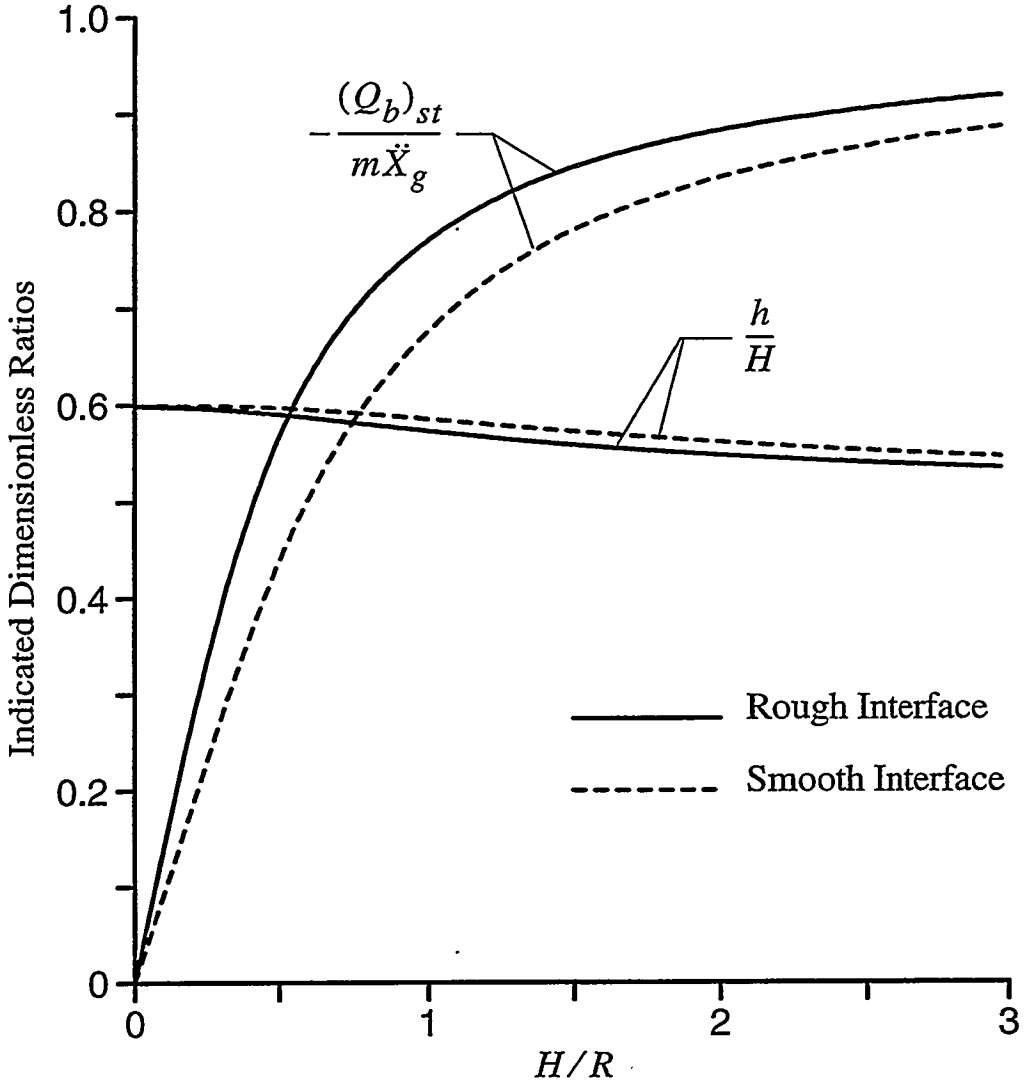

Fig. 4.3 Effect of Slenderness Ratio, H/R, on Static Value of Base Shear in Tank Wall and on Associated Effective Height; $\nu = 1/3$.

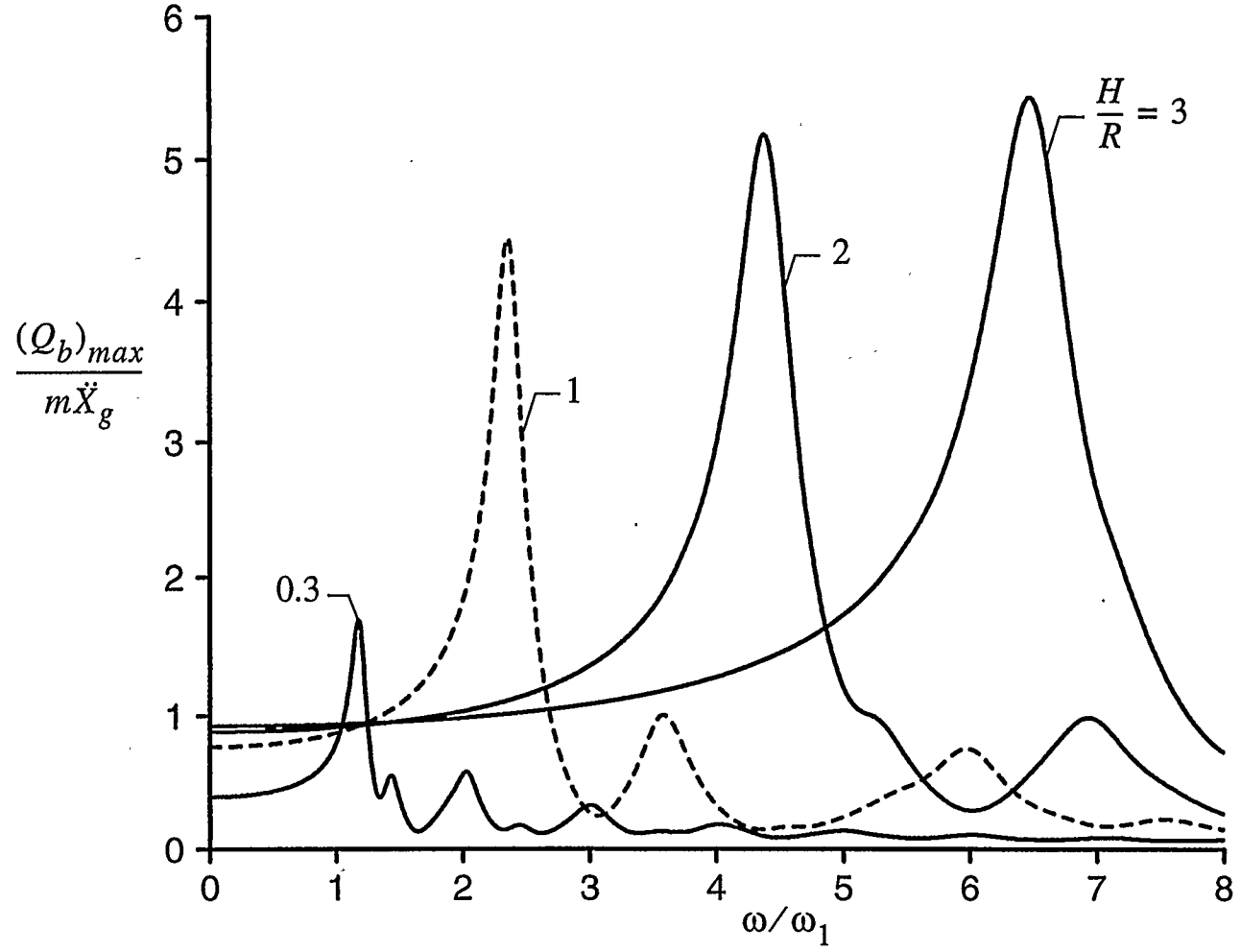

Fig. 4.4 Effect of Slenderness Ratio, H/R, on Frequency Response Curves for Base Shear in Wall of Systems with Rough Interface; $\nu = 1/3, \delta = 0.1$.

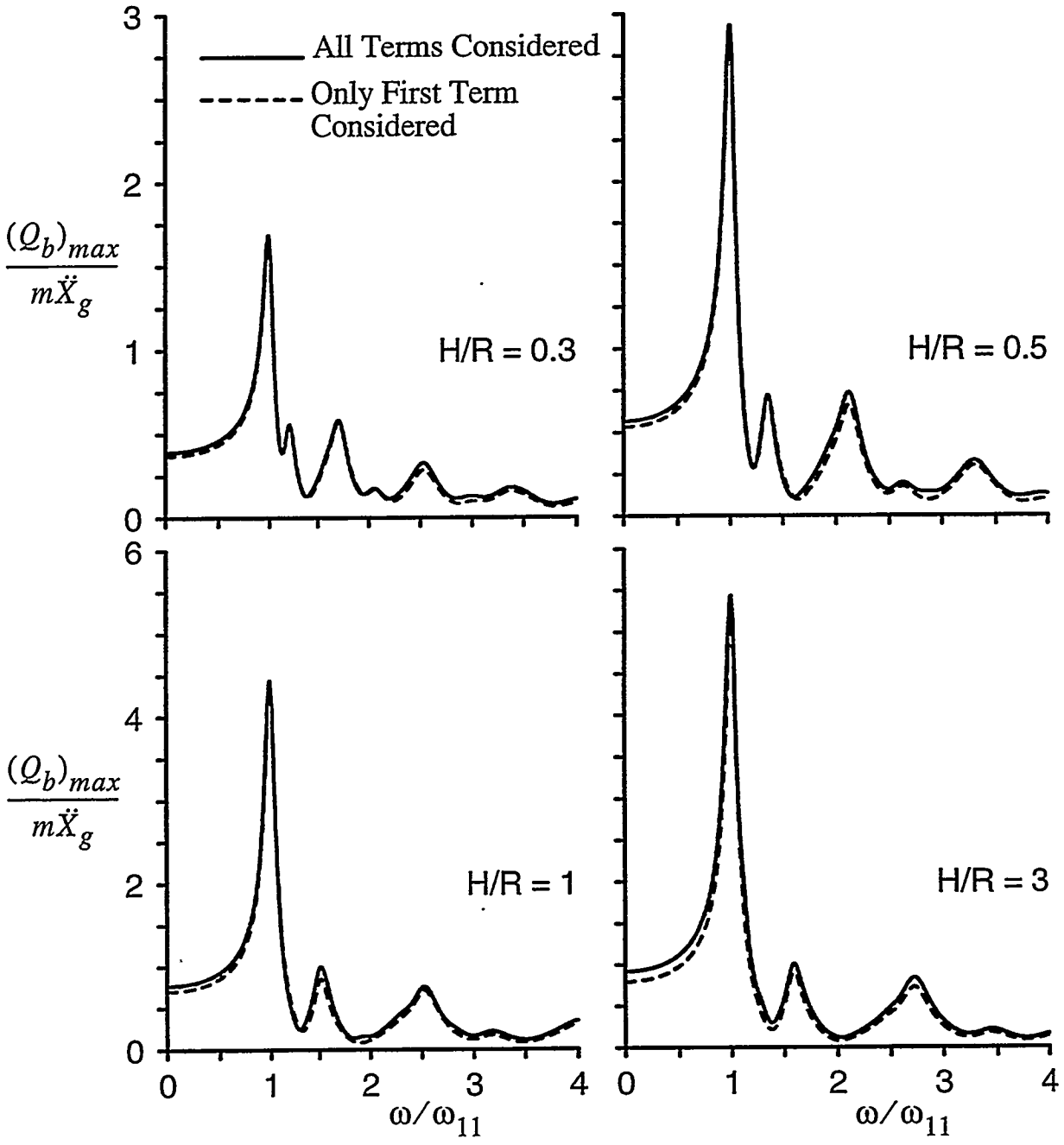

Fig. 4.5 Frequency Response Curves for Amplification Factors of Base Shear in Wall of Systems with Different Aspect Ratios Computed Using Only First and All Terms in Series; Rough Interface, $\nu = 1/3$, $\delta = 0.1$.

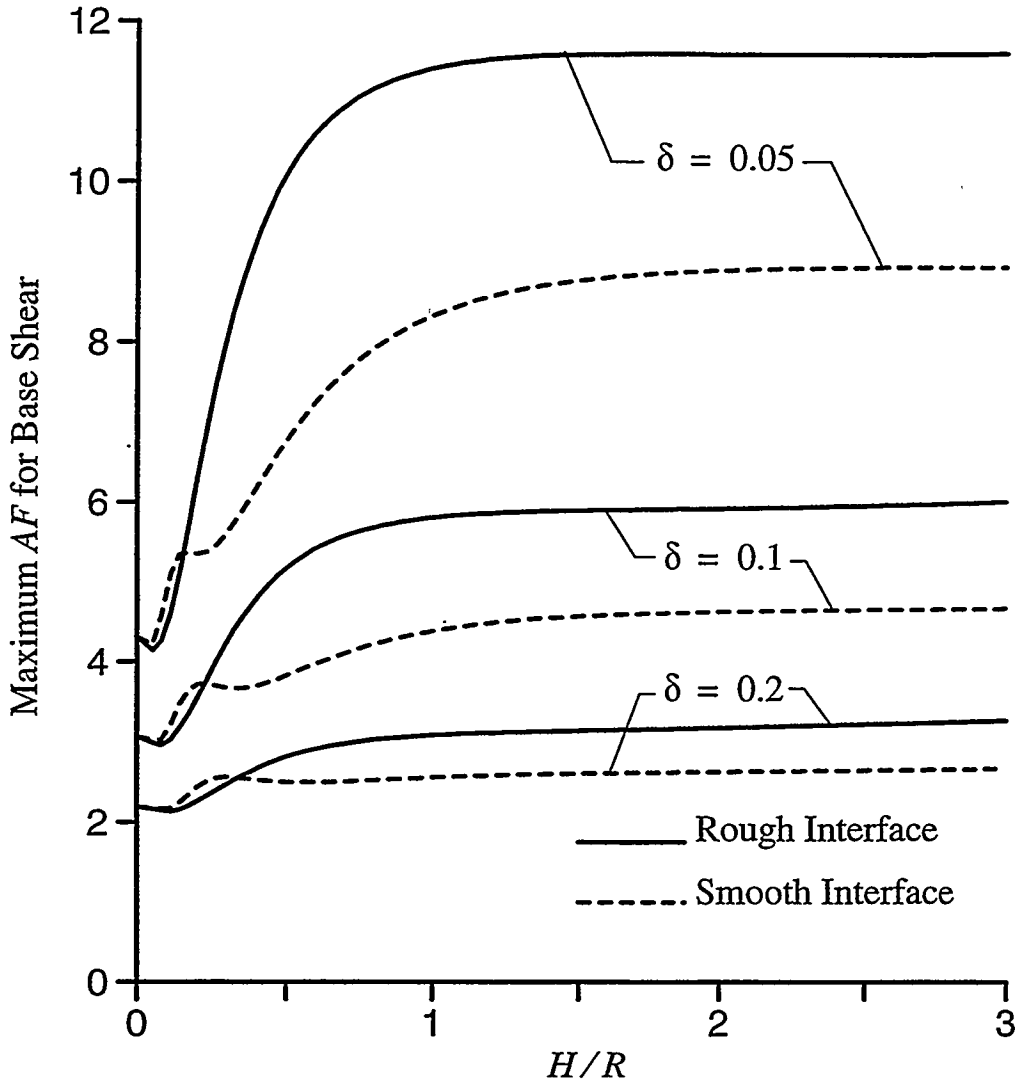

Fig. 4.6 Maximum Amplification Factor for Base Shear in Wall of Harmonically Excited Systems; $\nu = 1/3$, $\delta = 0.1$.

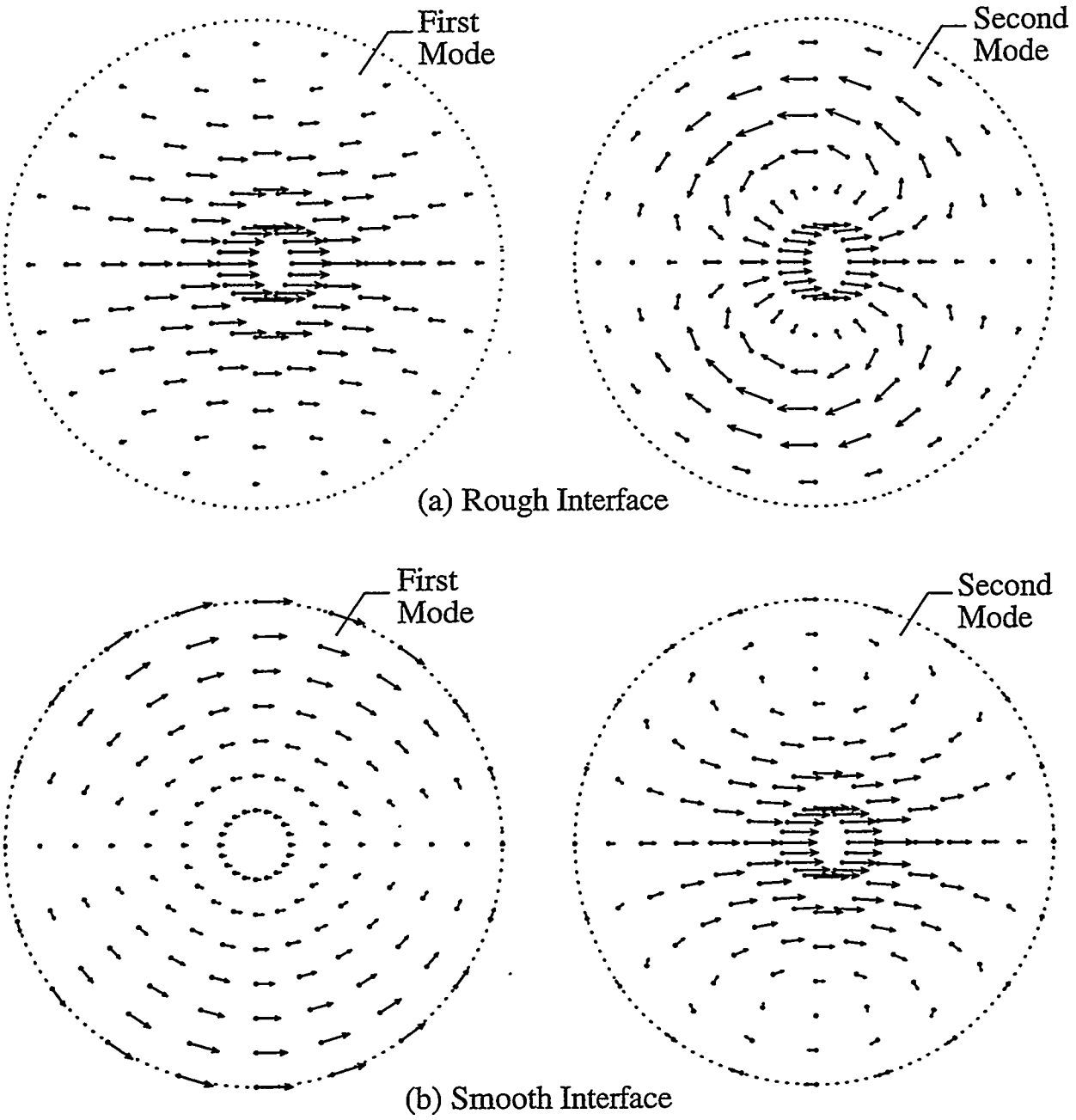

Fig. 4.7 Distributions of Inertia Forces for First Two Horizontal Natural Modes of Vibration of Material in Tanks with Rough and Smooth Wall Interfaces; $\nu = 1/3$.

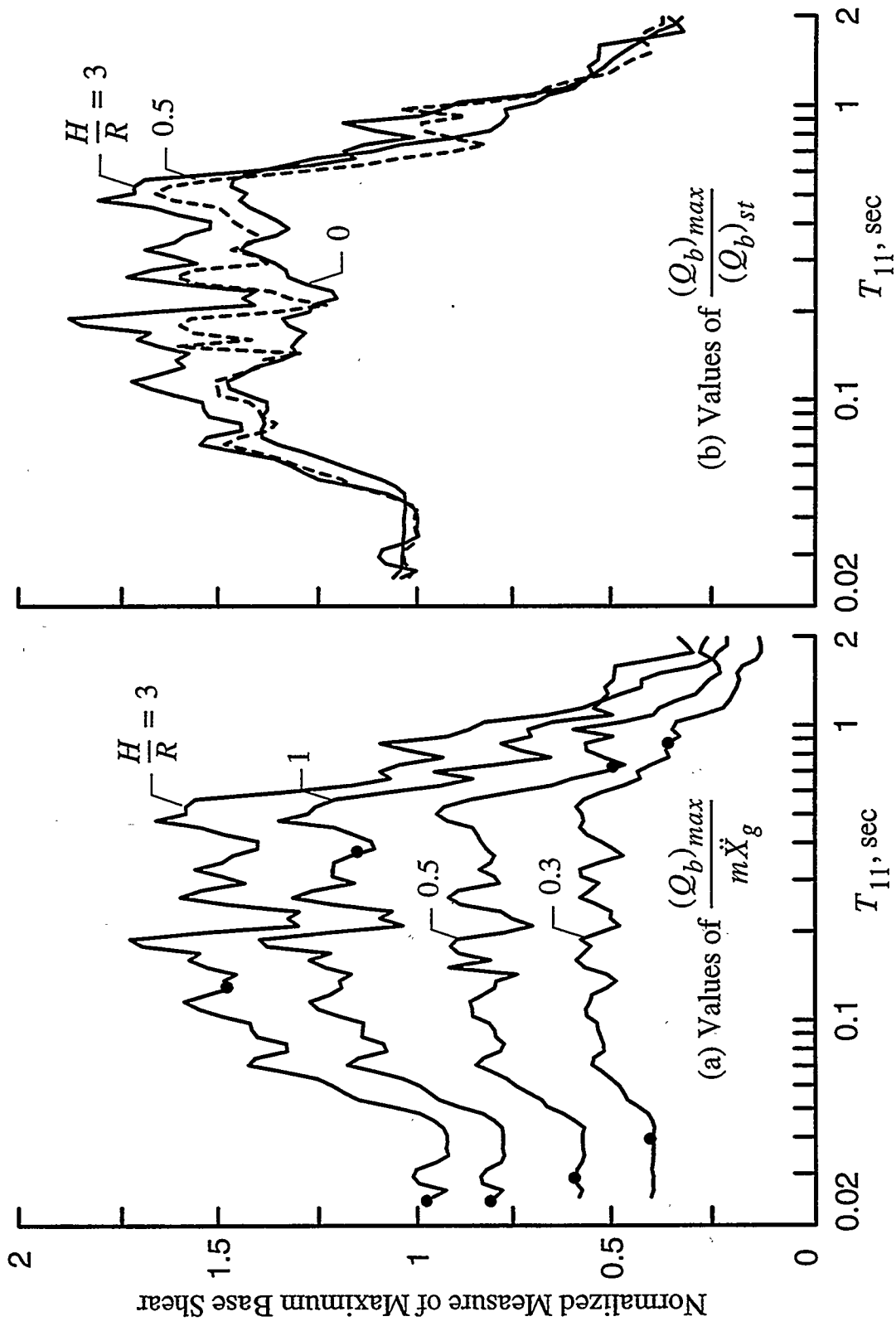

Fig. 4.8 Normalized Values of Base Shear in Systems with Different Aspect Ratios Subjected to El Centro Ground Motion Record; Rough Wall Interface, $\nu = 1/3$, $\delta = 0.1$.

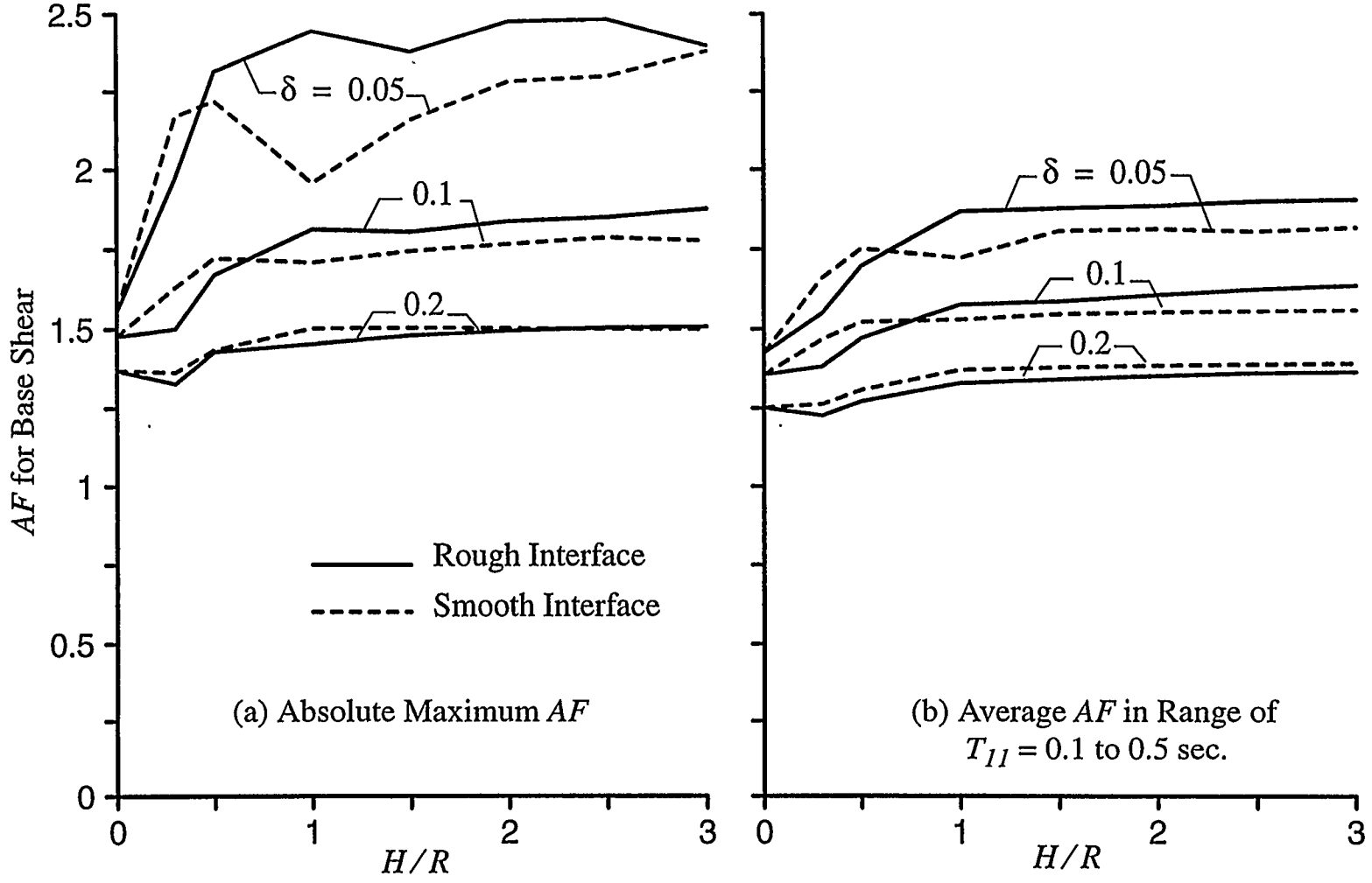

Fig. 4.9 Absolute Maximum and Average Amplification Factors for Base Shear in Wall of Systems Subjected to El Centro Ground Motion Record; $\nu = 1/3$, $\delta = 0.1$; Average Taken over Period Range from $T_{11} = 0.1$ to 0.5 sec.

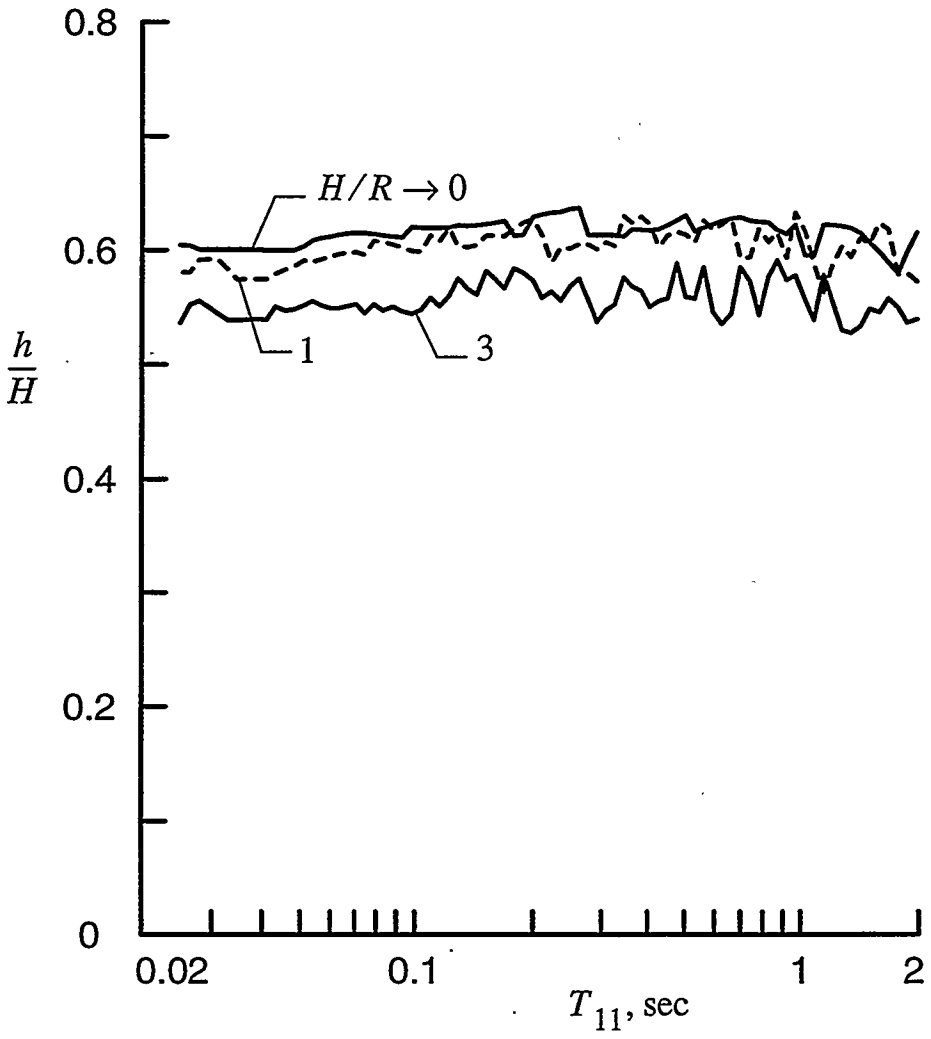

Fig. 4.10 Normalized Effective Heights of Systems Subjected to El Centro Ground Motion Record; Rough Wall Interface, $\nu = 1/3$, $\delta = 0.1$.

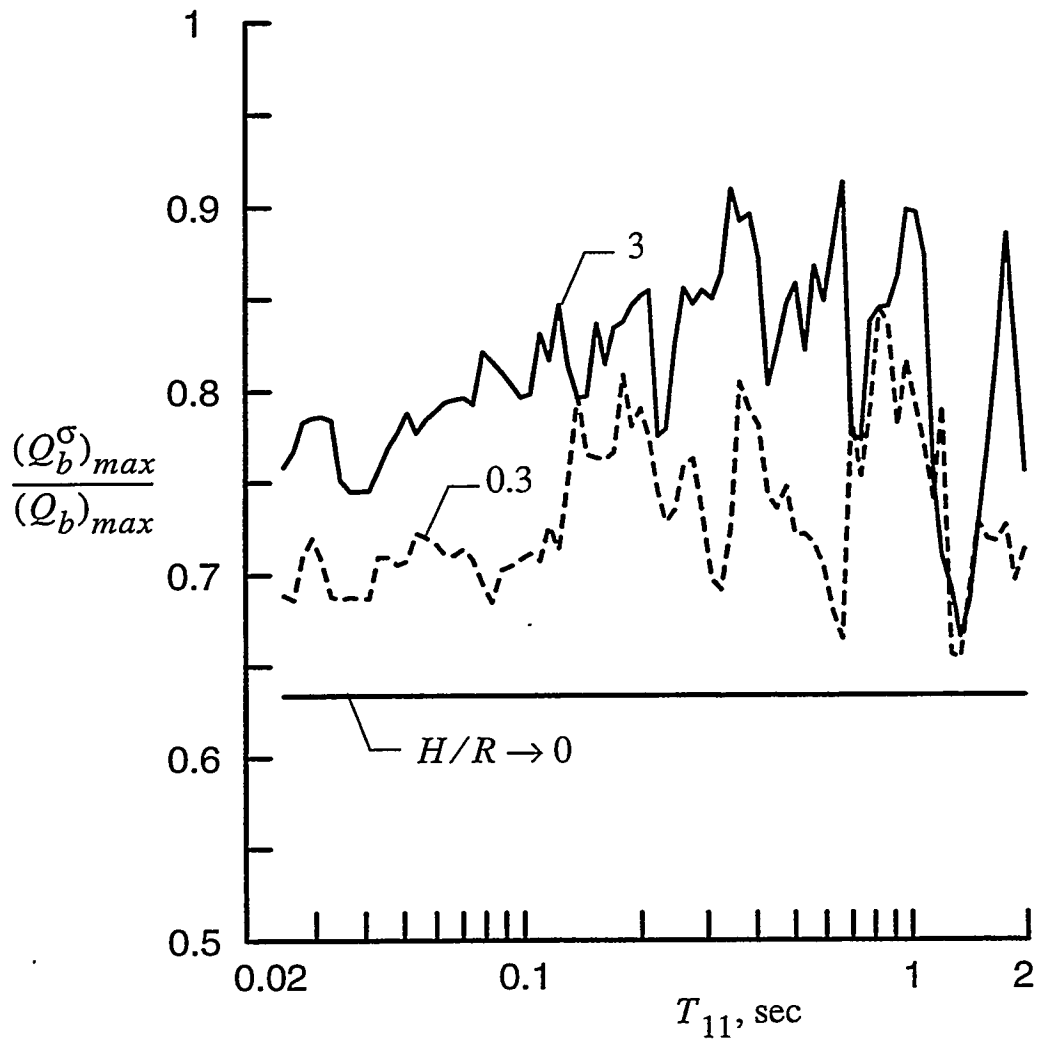

Fig. 4.11 Fraction of Total Base Shear in Wall of Systems with Rough Interface Induced by Normal Wall Pressures; Systems with $\nu = 1/3$ and $\delta = 0.1$ Subjected to El Centro Ground Motion Record.

SECTION 5

FOUNDATION FORCES

For the design of the tank foundation, one needs to know the total shear and total overturning moment transmitted to it. The foundation shear is clearly equal to the sum of the base shear in the tank wall and the shear at the base of the contained material. Similarly, the foundation moment equals the sum of the base moments induced by the wall pressures and those acting on the tank base. Considering that the method of analysis employed presumes the absence of any vertical dynamic pressures, the component of the moment contributed by the base pressures cannot be computed. However, both the foundation shear $\tilde{Q}$ and the foundation moment $\tilde{M}$ can be determined directly from the lateral inertia forces. In particular, their static values are given by

$$\tilde{Q}_{st} = -m\ddot{X}_g \tag{50}$$

$$\tilde{M}_{st} = -\frac{1}{2}m\ddot{X}_g H \tag{51}$$

and the maximum dynamic values are given by the products of their corresponding static values and appropriate amplification factors. To a reasonable degree of approximation, the amplification factors may be taken equal to those for the base shear in the tank wall. This approximation is considered to be adequate for both harmonic and transient excitations. With the foundation shear $\tilde{Q}$ and the foundation moment $\tilde{M}$ established, the components contributed by the dynamic stresses at the tank base may, if desired, be determined by substracting from $\tilde{Q}$ the base shear in the tank wall Q_b, and from $\tilde{M}$ the base moment M_b due to the wall pressures.

The instantaneous values of the foundation shear and overturning moment can more accurately be computed from

$$\tilde{Q} = -\int_V \rho[\ddot{x}_g + \ddot{u}_x]\, dV \tag{52}$$

$$\tilde{M} = -\int_V \rho[\ddot{x}_g + \ddot{u}_x]\, z\, dV \tag{53}$$

in which $\ddot{u}_x$ = the acceleration relative to the moving base of an arbitrary point of the contained material in the direction of the base motion (i.e., along $\theta = 0$), and the integration is over the volume of the contained material. For a harmonic excitation, (52) and (53) can be rewritten as

$$\tilde{Q} = -\int_0^1 \int_0^1 \int_0^{2\pi} [\rho \ddot{X}_g - \omega^2 U_x] d\theta \, R^2 \xi d\xi H d\eta \; e^{i\omega t} \tag{54}$$

$$\tilde{M} = -\int_0^1 \int_0^1 \int_0^{2\pi} [\rho \ddot{X}_g - \omega^2 U_x] d\theta \, R^2 \xi d\xi \, H^2 \eta d\eta \; e^{i\omega t} \tag{55}$$

where U_x, the amplitude of the horizontal displacement relative to the moving base, is given by

$$U_x = U\cos\theta - V\sin\theta \tag{56}$$

and U and V are the corresponding amplitudes of the radial and circumferential displacements, which are defined by (19) and (20), respectively. On making use of (19), (20) and (56), and performing the indicated integrations, one obtains

$$\frac{\tilde{Q}}{\tilde{Q}_{st}} = \left\{1 + \frac{8}{\pi^2}\left(\frac{\omega}{\omega_1}\right)^2 \sum_{n=1}^{\infty} \frac{1}{(2n-1)^4} \frac{[1 - A_n I_1(\alpha_n) - B_n I_1(\beta_n)]}{1 - \phi_n^2 + i\delta}\right\} e^{i\omega t} \tag{57}$$

$$\frac{\tilde{M}}{\tilde{M}_{st}} = \left\{1 + \frac{32}{\pi^3}\left(\frac{\omega}{\omega_1}\right)^2 \sum_{n=1}^{\infty} \frac{(-1)^{n+1}}{(2n-1)^5} \frac{[1 - A_n I_1(\alpha_n) - B_n I_1(\beta_n)]}{1 - \phi_n^2 + i\delta}\right\} e^{i\omega t} \tag{58}$$

where the integrations constants A_n and B_n are defined by (33a) and (33b) for a rough interface and by (34a) and (34b) for a smooth interface.

With the harmonic response established, the response to an arbitrary transient excitation may be determined, as for all other response quantities considered, by Fourier transform techniques.

SECTION 6

FINAL COMMENTS

Fundamental to the analysis presented has been the assumption that the material in the tank is bonded to its base. This assumption is justified by the fact, that for realistic intensities of ground shaking, the maximum shearing stress at the interface of the contained material and the tank base can be shown to be lower than the corresponding shearing capacity.

Finally, the base shears and base moments presented in the preceding section represent exclusively the effects of the normal pressures and circumferential shearing stresses induced by the inertia forces of the contained material. To these effects, must also be added the effects of the tank wall inertia. For the rigid tank considered, the latter effects, identified with a *w* superscript, are given simply by

$$Q_b^w = -m_w \ddot{X}_g \tag{59}$$

$$M_b^w = -\frac{1}{2} m_w \ddot{X}_g H \tag{60}$$

in which m_w = the total mass of the tank wall.

SECTION 7

CONCLUSIONS

Following are some of the more important conclusions of this study.

1. With the information that has been presented, the response to horizontal ground shaking of rigid circular cylindrical tanks containing a viscoelastic material may be evaluated readily. The comprehensive numerical data included provide valuable insights not only into the magnitude and distribution of the wall pressures and the magnitude of the critical forces, but also a valuable framework for the interpretation of the results for the flexible tanks examined in Part B of the report.
2. The maximum value of a dynamic effect is expressed as the product of the corresponding 'static' effect and an amplification factor. The 'static' effects, which refer to those induced by uniform lateral inertial forces equal in magnitude to the product of the mass density of the contained material and the maximum ground acceleration, depend on the ratio of the material height H and the tank radius R. For slender tanks with values of H/R greater than about 3, the inertia forces for all of the contained material are transmitted to the wall by horizontal extensional action, and practically the entire contained mass may be considered to be effective. With decreasing H/R, a progressively larger portion of the inertia forces gets transferred by horizontal shearing action to the base, and the portion of the retained mass that contributes to the wall forces is reduced significantly.
3. For a system of a specified H/R, the dynamic amplification factor depends importantly on the fundamental natural period of the contained material. This dependence is similar to, but by no means identical to, that obtained for a similarly excited, viscously damped single-degree-of-freedom oscillators. Specifically, for low-natural-period, stiff materials, the amplification factor is unity. With increasing flexibility or period of the contained material, the amplification factor increases and after attaining a nearly horizontal plateau, which for broad-banded earthquake ground motions may be of the order of 1.25 to 2.5, it decreases, reaching values less than unity. The larger amplification factors are attained for the slender tanks and for materials with low damping.
4. Because of the assumption of vanishing vertical normal stresses that underlies the simplified method of analysis employed, the component of the foundation moment contributed by the dynamic pressures acting on the tank base cannot be evaluated. However, the total foundation moment and shear may be determined directly from the inertia forces of the retained medium.

SECTION 8

APPENDIX: UNDAMPED FREE VIBRATION OF CONTAINED SOLID

The natural modes of vibration considered here are those for which the radial displacements u vary in the circumferential direction as $\cos\theta$ and the circumferential displacements v vary as $\sin\theta$. For the excitation considered, these are the only modes that contribute to the response of the system. These displacements may be expressed as

$$u(\xi, \theta, \eta, t) = \mathcal{U}(\xi) \sin\left[\frac{(2n-1)\pi}{2}\eta\right] \cos\theta \; e^{i\omega t} \tag{61}$$

$$v(\xi, \theta, \eta, t) = \mathcal{V}(\xi) \sin\left[\frac{(2n-1)\pi}{2}\eta\right] \sin\theta \; e^{i\omega t} \tag{62}$$

and the functions $\mathcal{U}(\xi)$ and $\mathcal{V}(\xi)$ may be determined by application of the decoupling technique used in the body of the paper. The results are

$$\mathcal{U}(\xi) = \mathcal{A}\left[\alpha I_0(\alpha\xi) - \frac{1}{\xi} I_1(\alpha\xi)\right] + \mathcal{B}\,\frac{1}{\xi} I_1(\beta\xi) \tag{63}$$

$$\mathcal{V}(\xi) = -\mathcal{A}\,\frac{1}{\xi} I_1(\alpha\xi) - \mathcal{B}\left[\beta I_0(\beta\xi) - \frac{1}{\xi} I_1(\beta\xi)\right] \tag{64}$$

where $\mathcal{A}$ and $\mathcal{B}$ are constants of integration, and the dimensionless frequency parameters α and β are defined by specialized forms of (25) and (26) as

$$\alpha = \frac{\beta}{\psi_o} \tag{65}$$

$$\beta = \frac{(2n-1)\pi}{2}\frac{R}{H}\sqrt{1 - \frac{\omega^2}{\omega_n^2}} \tag{66}$$

On satisfying the boundary conditions defined by (12) and either (13) or (14), and setting the determinant of the coefficients of the resulting system of homogeneous equations in $\mathcal{A}$ and $\mathcal{B}$ equal to zero, one obtains the characteristic equation of the system. The frequency ω corresponding to the mth root of the latter equation is denoted by ω_{mn}, and the corresponding values of α, β, $\mathcal{A}$, $\mathcal{B}$ and functions $\mathcal{U}(\xi)$ and $\mathcal{V}(\xi)$ are identified with the subscript m.

Inasmuch as the values of ω_{mn} corresponding to a given n are greater than ω_n, the associated values of α_m and β_m are imaginary, and it is convenient to rewrite α as $i\gamma$ and β as $i\psi_o\gamma$ where γ is a real-valued number. On further noting that

$$I_0(i\gamma) = J_0(\gamma) \tag{67}$$

$$I_1(i\gamma) = i\,J_1(\gamma) \tag{68}$$

where J_0 and J_1 are Bessel functions of the first type and zero and first order, respectively, the characteristic equation for a system with a rough interface becomes

$$\psi_o\gamma\,J_0(\gamma)\,J_0(\psi_o\gamma) - J_0(\gamma)\,J_1(\gamma) - \psi_o\,J_0(\psi_o\gamma)\,J_1(\gamma) = 0 \tag{69}$$

and that for a smooth interface becomes

$$\left[\gamma\,J_0(\gamma) - J_1(\gamma)\right]\left[2\,\psi_o\gamma\,J_0(\psi_o\gamma) + (\psi_o\gamma)^2\,J_1(\gamma)\right] - 2\gamma J_0(\gamma)J_1(\psi_o\gamma) = 0 \tag{70}$$

With the roots γ_m and the corresponding values of α_m determined, the natural frequencies ω_{mn} are determined from (65) or (49), and the relative magnitudes of the constants $\mathcal{A}_m$ and $\mathcal{B}_m$ in (63) or (64) are determined from the expressions for the boundary conditions on $\mathcal{U}_m$ and $\mathcal{V}_m$. The values of $\mathcal{A}_m$ and $\mathcal{B}_m$ corresponding to the first five values of γ_m are listed in Table 4.2 normalized such that $\mathcal{U}_m$ at $\xi = 0$ is unity.

SECTION 9

REFERENCES

Pais, A., and Kausel, E. (1988). "Approximate formulas for dynamic stiffnesses of rigid foundations." *Soil Dyn. & Earthquake Eng.,* 7(4), 213-277.

Roesset, J. M., Whitman, R. V., and Dobry, R. (1973). "Modal analysis for structures with foundation interaction." *J. Struct. Div. ASCE,* 99 (3), 399-416.

Rotter, J. M., and Hull, T. S. (1989). "Wall loads is squat steel silos during earthquakes." Engineering Structures, 11, 139-147.

Tajimi, H. (1969). "Dynamic Analysis of a Structure Embedded in an Elastic Stratum," *Proc. of 4th World Conf. on Earthquake Eng.*, San Diego, Chile, IAEE, Tokyo, Japan, III(A-6), 53-69.

Veletsos, A. S., and Dotson, K. W. (1988). "Horizontal impedances for radially inhomogeneous viscoelastic soil layers." *Earthquake Eng. & Struct. Dyn.*, 16 (7), pp. 947-966.

Veletsos, A. S., Parikh, V. P., and Younan, A. H. (1995). "Dynamic response of a pair of long walls retaining a viscoelastic solid," *Earthquake Eng. & Struct. Dyn.*, 24 (12), pp. 1567-1589; also available as *Report 52454*, Brookhaven National Laboratory, Upton, N.Y.

Veletsos, A. S., and Tang, Y. (1990). "Deterministic assessment of effects of ground motion incoherence." *J. Eng. Mech. ASCE*, 116(5), pp. 1109-1124.

Veletsos, A. S., and Verbic, B. (1973). "Vibration of viscoelastic foundations." *Earthquake Eng. & Struct. Dyn.*, 2 (1), pp. 87-102.

Veletsos, A. S., and Younan, A. H. (1994a). "Dynamic soil pressures on rigid cylindrical vaults." *Earthquake Eng. & Struct. Dyn.*, 23 (6), pp. 645-669; also available as *Report 52372*, Brookhaven National Laboratory, Upton, N.Y.

Veletsos, A. S., and Younan, A. H. (1994b). "Dynamic modeling and response of soil-wall systems." *J. Geotech. Eng. ASCE*, 120 (12), pp. 2155-2179; also available as *Report 52402*, Brookhaven National Laboratory, Upton, N.Y.

PART B. FLEXIBLE TANKS

SECTION 1
INTRODUCTION

The study reported here is an extension of that presented in Part A. It deals with the effects of wall flexibility on the response to horizontal ground shaking of vertical, circular cylindrical tanks containing a uniform viscoelastic solid. The analysis is implemented approximately considering the tank wall to respond as a cantilever shear-beam with no change in its cross section.

The expressions for the critical responses of these systems are formulated, and comprehensive numerical data are presented that elucidate the effects of the numerous parameters involved. The principal parameters examined include the flexibility of the wall relative to that of the contained material, the ratio of material height to tank radius, and the characteristics of the forcing function. In addition to long-period, effectively static excitations, both harmonic motions of different frequencies and an actual earthquake ground motion are considered.

The principal effects of wall flexibility may be anticipated from purely physical considerations. Since the effective horizontal extensional stiffness of the retained material for a flexible tank is lower than that for a rigid tank, the flexibility of the wall should reduce the portion of the inertia forces transmitted to it by horizontal extensional action and increase the portion transmitted to the base by shearing action. Additionally, the wall flexibility should decrease the natural frequency of the tank-solid system and modify its effective damping. Depending on the characteristics of the system and the base motion, the latter changes may increase or decrease the critical responses from those obtained for a rigid tank. The primary objective of the study is to quantify these changes over the full range of the parameters involved. A secondary objective is to assess the relationship of these responses to those obtained for tanks containing an inviscid liquid of the same mass density. The maximum values of the critical responses are expressed as the products of those obtained under 'static' conditions of loading and appropriate amplification or deamplification factors.

As indicated in Part A, the only known previous study of solid-containing tanks is the one reported by Rotter and Hull (1989), which dealt with long-period, effectively static excitations.

SECTION 2

SYSTEM CONSIDERED

Except for considering the tank wall to be flexible, the system examined is the same as that studied in Part A. It is a vertical, circular cylindrical tank of radius R that is filled to a height H with a homogeneous, linear viscoelastic solid. The tank is presumed to be fixed to a rigid base undergoing a space-invariant horizontal motion, the acceleration of which at any time t is $\ddot{x}_g(t)$ and its maximum value is $\ddot{X}_g$. The contained medium is considered to be free at its upper surface and bonded at the base and along its cylindrical boundary.

The properties of the medium are defined by its mass density ρ, Poisson's ratio ν, and the complex-valued shear modulus $G^* = G(1 + i\delta)$, where G is the real-valued modulus, $i = \sqrt{-1}$, and δ is the damping factor, which is twice as large as the coefficient of damping normalized with respect to its critical value. The corresponding properties of the tank wall are denoted by ρ_w, ν_w, and $G_w^* = G_w(1 + i\delta_w)$, and the wall is considered to be of uniform thickness t_w. Points in the contained medium are defined by the cylindrical coordinate system, r, θ, z, the origin of which is taken at the center of the tank base, with θ measured counterclockwise from the direction of the excitation.

SECTION 3

METHOD OF ANALYSIS

The method of analysis used is an extension of that described in Part A for rigid tanks and involves all the previously noted assumptions and approximations. It is further assumed that the tank wall responds as a cantilever shear-beam with no change in its cross section, and that there is complete bonding between the contained medium and the wall. It follows that along its cylindrical boundary, the radial and circumferential displacements of the medium relative to the moving base, u and v, are given by

$$u|_{\xi=1} = u_w(\eta, t)\cos\theta \tag{1}$$

and

$$v|_{\xi=1} = -u_w(\eta, t)\sin\theta \tag{2}$$

where $\xi = r/R$ and $\eta = z/H$ are dimensionless position coordinates, and u_w = the displacement relative to the base of an arbitrary point of the wall in the direction of the excitation.

3.1 Harmonic Response

For a harmonic base motion for which the acceleration

$$\ddot{x}_g(t) = \ddot{X}_g e^{i\omega t} \tag{3}$$

and ω is its circular frequency, the steady-state values of the displacements u and v of an arbitrary point in the contained medium may be expressed, as for a rigid tank, in the form

$$u(\xi, \theta, \eta, t) = \sum_{n=1}^{\infty} U_n(\xi)\sin\left[\frac{(2n-1)\pi}{2}\eta\right]\cos\theta\, e^{i\omega t} \tag{4}$$

$$v(\xi, \theta, \eta, t) = \sum_{n=1}^{\infty} V_n(\xi)\sin\left[\frac{(2n-1)\pi}{2}\eta\right]\sin\theta\, e^{i\omega t} \tag{5}$$

and the corresponding tank wall displacement, u_w, may be expressed as

$$u_w(\eta, t) = \sum_{n=1}^{\infty} U_n^w \sin\left[\frac{(2n-1)\pi}{2}\eta\right] e^{i\omega t} \tag{6}$$

where U_n^w are constants that remain to be determined.

On expanding the unit function associated with the ground acceleration terms in the equations of motion defined by (8) and (9) of Part A in the form

$$1 = \frac{4}{\pi}\sum_{n=1}^{\infty}\frac{1}{2n-1}\sin\left[\frac{(2n-1)\pi}{2}\eta\right] \tag{7}$$

substituting (4) and (5) into the latter equations and satisfying the boundary conditions defined by (1) and (2), with u_w expressed as in (6), the functions U_n and V_n can be shown to be given by

$$U_n(\xi) = U_n^f - \left\{ A_n\left[\alpha_n I_0(\alpha_n\xi) - \frac{1}{\xi} I_1(\alpha_n\xi)\right] + B_n\frac{1}{\xi} I_1(\beta_n\xi)\right\}\{U_n^f - U_n^w\} \tag{8}$$

and

$$V_n(\xi) = -U_n^f + \left\{ A_n\frac{1}{\xi} I_1(\alpha_n\xi) + B_n\left[\beta_n I_0(\beta_n\xi) - \frac{1}{\xi} I_1(\beta_n\xi)\right]\right\}\{U_n^f - U_n^w\} \tag{9}$$

where I_0 and I_1 are modified Bessel functions of the first kind and zero and first order, respectively, and the remaining quantities are the same as those in the corresponding expressions for rigid tanks. Specifically, α_n and β_n are defined by (25) and (26) of Part A, and U_n^f, A_n and B_n by (29), (33a) and (33b) of the same part.

Wall Stresses and Associated Forces

The radial or normal pressures σ_r and the circumferential shearing stresses $\tau_{r\theta}$ induced on the cylindrical wall may be expressed as

$$\sigma_r(\eta, \theta, t) = \sigma(\eta)\cos\theta\, e^{i\omega t} = \sum_{n=1}^{\infty}(\sigma_r)_n \sin\left[\frac{(2n-1)\pi}{2}\eta\right]\cos\theta\, e^{i\omega t} \tag{10}$$

$$\tau_{r\theta}(\eta, \theta, t) = \tau(\eta)\sin\theta\, e^{i\omega t} = \sum_{n=1}^{\infty}(\tau_{r\theta})_n \sin\left[\frac{(2n-1)\pi}{2}\eta\right]\sin\theta\, e^{i\omega t} \tag{11}$$

where $\sigma(\eta)$ and $\tau(\eta)$ and the amplitudes of their components, $(\sigma_r)_n$ and $(\tau_{r\theta})_n$, are complex-valued quantities. On noting that U_n^f in (8) and (9) is independent of ξ, and that the terms

$$\frac{1}{\xi}\frac{\partial v}{\partial\theta} + \frac{u}{\xi} \quad \text{and} \quad \frac{1}{\xi}\frac{\partial u}{\partial\theta} + \frac{v}{\xi}$$

in the expressions for σ_r and $\tau_{r\theta}$ [equations (4) and (6) in Part A] vanish along the medium-wall interface, it should be clear that $(\sigma_r)_n$ and $(\tau_{r\theta})_n$ may be determined from the corresponding terms in the solution for rigid tanks simply by multiplying the nth term of the appropriate expression in the latter solution by the reduction factor

$$R_n = 1 - \frac{U_n^w}{U_n^f} \tag{12}$$

The sign convention for stresses is the same as that in Part A. Specifically, normal pressures are considered positive when tensile, and the positive directions of the shearing stresses are shown by the inset diagrams in Fig. 2.1 of Part A. The nth components of the total wall force and of the overturning moment at a section immediately above the base may be determined similarly from the corresponding components for rigid tanks.

The as yet undetermined reduction factors R_n, and hence the values of U_n^w/U_n^f, are computed by considering the horizontal equilibrium of forces acting on a wall section of unit height. This requires that

$$F_i(\eta) + F_s(\eta) + F_c(\eta) = 0 \tag{13}$$

where F_i = the wall inertia force, F_s = the resisting shearing force, and F_c = the force exerted by the contained medium. These forces are given by

$$F_i = -2\pi R t_w \rho_w (\ddot{u}_w + \ddot{x}_g) \tag{14}$$

$$F_s = 2\pi R t_w \frac{1}{H}\frac{\partial \tau_{zx}}{\partial \eta} = 2\pi R t_w \frac{G_w^*}{H^2}\frac{\partial^2 u_w}{\partial \eta^2} \tag{15}$$

and

$$F_c = \int_0^{2\pi} (\tau \sin^2\theta - \sigma\cos^2\theta) R d\theta \, e^{i\omega t} = \pi R(\tau - \sigma)\, e^{i\omega t} \tag{16}$$

where a dot superscript denotes one differentiation with respect to time, and τ_{zx} represents the horizontal shearing stress in the direction of the base motion. On substituting (14) through (16) into (13), making use of (6) and of the expressions for the reduced versions of $\sigma(\eta)$ and $\tau(\eta)$, the factor R_n is found to be given by

$$R_n = \frac{\dfrac{1+i\delta_w}{1+i\delta} - d_w\dfrac{m_w}{m}}{\dfrac{1+i\delta_w}{1+i\delta} - d_w\dfrac{m_w}{m}\dfrac{\phi_n^2}{1+i\delta} - d_w C_n} \tag{17}$$

where $\phi_n = \omega/\omega_n$; ω_n = the nth circular frequency of the contained material when it is considered to act as an unconstrained, cantilever shear-beam, given by

$$\omega_n = \frac{(2n-1)\pi}{2}\frac{v_s}{H} \tag{18}$$

$v_s = \sqrt{G/\rho}$ = shear wave velocity of the retained material; m_w/m = ratio of masses of the tank wall and the contained material, given by

$$\frac{m_w}{m} = 2\frac{\rho_w}{\rho}\frac{t_w}{R} \tag{19}$$

d_w is a dimensionless measure of the wall flexibility, defined by

$$d_w = \frac{1}{2}\frac{GR}{G_w t_w} \tag{20}$$

and

$$C_n = \frac{2}{\pi}\frac{\psi_o g_n + h_n}{2n-1}\frac{H}{R}\sqrt{\frac{1-\phi_n^2+i\delta}{1+i\delta}} \tag{21}$$

The quantities ψ_o, g_n and h_n in the latter expression are factors defined by (7), (39a) and (39b) of Part A.

Effect of Wall Inertia

The inertia of the tank wall has a two-fold effect: (a) It modifies the magnitude and distribution of the dynamic wall pressures and associated forces; and (b) it induces additional forces in the wall. The first effect has duly been provided for in the evaluation of the reduction factors R_n, but the second has not been included in the expressions for base shear and base moment referred to in the preceding section.

The instantaneous values of the base shear and base moment induced by the wall inertia, $Q_b^w(t)$ and $M_b^w(t)$, are given by

$$Q_b^w(t) = -2\pi R t_w \rho_w \int_0^1 (\ddot{u}_w + \ddot{x}_g) H d\eta \tag{22a}$$

and

$$M_b^w(t) = -2\pi R t_w \rho_w \int_0^1 (\ddot{u}_w + \ddot{x}_g) H^2 \eta d\eta \tag{22b}$$

which, on making use of (3), (6) and (12), reduce to

$$Q_b^w(t) = -m_w \ddot{X}_g \left[1 + \frac{8}{\pi^2}\left(\frac{\omega}{\omega_1}\right)^2 \sum_{n=1}^{\infty} \frac{1}{(2n-1)^4}\frac{1-R_n}{1-\phi_n^2+i\delta}\right] e^{i\omega t} \tag{23a}$$

and

$$M_b^w(t) = -\frac{1}{2} m_w \ddot{X}_g H\left[1 + \frac{32}{\pi^3}\left(\frac{\omega}{\omega_1}\right)^2 \sum_{n=1}^{\infty} \frac{(-1)^{n-1}}{(2n-1)^5} \frac{1-R_n}{1-\phi_n^2+i\delta}\right] e^{i\omega t} \qquad (23b)$$

respectively. For a rigid tank, the reduction factors R_n tend to unity; the terms that include these factors vanish; and the amplitudes of the base shear and base moment reduce, as they should, to $m_w\ddot{X}_g$ and $m_w\ddot{X}_g H/2$, respectively.

3.2 Transient Excitation

The response to an arbitrary transient excitation may be evaluated from the harmonic response by the discrete Fourier transform (DFT) approach as outlined in Part A.

SECTION 4

CRITICAL RESPONSES OF SYSTEM

Following the approach used in the analysis of rigid tanks, consideration is first given to the response of systems subjected to long-period, effectively static excitations. The maximum value of a critical response to an arbitrary excitation may then be obtained by multiplying the corresponding 'static' value by an appropriate amplification or deamplification factor. Unless otherwise indicated, the mass of the wall in the solutions presented is considered to be negligible compared to the mass of the retained material, a condition normally satisfied in practice.

4.1 Static Effects

The static value of the base shear in the tank wall, $(Q_b)_{st}$, is plotted in Fig. 4.1 as a function of the relative flexibility factor d_w for systems with different slenderness ratios, H/R. It should be recalled that $d_w = 0$ refers to rigid tanks. The results are normalized with respect to the product of the total contained mass m and the maximum ground acceleration $\ddot{X}_g$, namely, the total inertia of the retained material when it is considered to act as a rigid body. Poisson's ratio for the contained material is taken as $\nu = 1/3$.

It is observed from Fig. 4.1 that the base shear, and hence the proportion of the contained mass contributing to this shear, is highly dependent on both the slenderness ratio H/R and the relative flexibility factor d_w. For rigid, tall tanks with values of H/R of the order of 3 or more, the inertia forces for all the retained material are effectively transmitted to the wall by horizontal shearing action, and practically the entire mass of the tank content may be considered to contribute to the wall force. With decreasing H/R, a progressively larger portion of the inertia forces gets transferred by horizontal shearing action to the base, and the effective portion of the retained mass is reduced.

The effect of wall flexibility is to reduce the horizontal extensional stiffness of the contained material relative to its shearing stiffness, and this reduction, in turn, reduces the magnitudes of the resulting pressures on and associated forces in the tank wall. The reduced response of the flexible tanks is in sharp contrast to the well established behavior of liquid-containing tanks, for which the effect of wall flexibility is to increase rather than decrease the impulsive components of the wall pressures and forces which dominate the response of such systems. This matter is considered further in a later section.

As for rigid tanks, the static value of the overturning base moment, , may be expressed as the product of the total wall force or base shear and an appropriate height, *h*. The variation of the ratio h/H for tanks with different values of d_w and H/R is shown in Fig. 4.2. Note that almost independently of the relative flexibility factor d_w, the effective height varies from 0.6*H* for broad tanks with values of H/R tending to zero to 0.5*H* for rather tall, slender tanks. This trend may be appreciated better from Fig. 4.3 which shows the heightwise variations of the normal wall pressures, $\sigma_{st}(\eta)$, for tanks of different proportions and flexibilities. It is observed that for broad tanks, these pressures increase from base to top approximately as a quarter-sine wave, whereas for the rather slender tanks, the distribution is practically uniform. The distributions of the corresponding horizontal shearing stresses $\tau_{st}(\eta)$ are similar and are not shown. The top values of these stresses for systems with different d_w and H/R values are listed in part (a) of Table 4.1. Also listed in this table are normalized values of the total wall force and its effective height.

4.2 Harmonic Response

The steady-state amplitude of the total wall force or base shear in the wall of harmonically excited systems, $(Q_b)_{max}$, is plotted in Fig. 4.4 as a function of the frequency ratio ω/ω_1 for systems with H/R = 1. Four values of the wall flexibility factor d_w in the range between zero and 3 are considered. The remaining parameters for the systems are identified on the figure heading.

As would be expected, the peak values of these plots are attained at or close to the undamped natural frequencies of the system considered, with the absolute maximum values occurring at the fundamental frequency. Denoted by ω_{11}, the latter frequency is quite sensitive to the wall flexibility factor. For highly flexible walls with values of $d_w \to \infty$, this frequency is practically equal, as it should be, to the natural frequency of the unconstrained medium ω_1; with decreasing wall flexibility, the frequency increases; and as $d_w \to 0$, it tends to the value for rigid tanks defined by equation (49) of Part A.

The fundamental natural frequency and the associated period of the system $T_{11} = 2\pi/\omega_{11}$ also depend on the slenderness ratio H/R. This dependence is shown in Fig. 4.5, in which the ratio T_{11}/T_1 is plotted as a function of the relative wall flexibility factor d_w for different values of H/R. Some of the data are also listed in Table 4.2. Note that the effect on T_{11} of a change in d_w is significantly larger for slender tanks than for broad tanks. As a matter of fact, for the limiting case of $H/R \to 0$, the results are independent of d_w.

In Fig. 4.6, the absolute maximum amplification factor for base shear, $(AF)_{max}$, defined as the ratio of the highest peak of a frequency response curve such as those displayed in Fig. 4.4 to the corresponding response of the statically excited system, is plotted as a function of the wall flexibility factor d_w for different values of H/R. The left-hand part of the figure is for systems with a damping factor for the tank wall $\delta_w = 0.04$, whereas the right-hand part is for systems with $\delta_w = 0.08$. All

other parameters are identified on the figure heading. It is observed that the amplification factors are generally quite large and sensitive to the values of H/R and d_w involved. The larger factors are obtained for the more slender and more flexible systems (larger values of H/R and d_w), indicating that their effective damping in this case is relatively low. System damping is contributed partly by the tank wall and partly by the hysteretic action of the contained material. The latter source dominates the response of broad tanks, while the wall damping dominates the response of slender tanks. This fact is clearly demonstrated by the interrelationship of the solutions for the two values of wall damping considered.

Further insight into the effect of wall flexibility may be gained from Fig. 4.7, where the information on the maximum response of systems examined in Fig. 4.6 is replotted with the absolute maximum value of the base shear amplitude, $|(Q_b)_{max}|$, normalized with respect to the common factor $m\ddot{X}_g$. Note that for the combination of parameters represented by points to the right of the heavy dots, the effect of wall flexibility is to reduce the response to levels that may be substantially lower than those applicable to rigid tanks. This reduction, which is due to the increased capacity of the material in flexible tanks to transfer the inertia forces by horizontal shearing action to the base, is, as already noted, in sharp contrast to the response of liquid-containing tanks, for which the effect of wall flexibility is to increase rather than decrease the response. Only for extremely slender tanks, for which the horizontal shearing stiffness of the contained material relative to its extensional stiffness is negligible as for a liquid, does the wall flexibility increase the response. For the range of parameters normally encountered in practice, the dynamic forces for tanks storing a viscoelastic material can be expected to decrease with increasing wall flexibility. Similar results, but with substantially lower response levels, can also be expected for transient excitations.

4.3 Seismic Response

Figure 4.8 shows the amplification factor for the base shear, *AF*, in the wall of systems subjected to the N-S component of the 1940 El Centro, California earthquake ground motion record. Three values of the slenderness ratio H/R and three values of the wall flexibility factor d_w are considered. The results are plotted as a function of the fundamental natural period $T_{11} = 2\pi/\omega_{11}$ of the system under consideration, which may be determined from the information presented in Table 4.2. As before, the tank wall in these solutions is presumed to be massless; Poisson's ratio and the damping factor of the retained material are taken as $\nu = 1/3$ and $\delta = 0.1$; and the damping factor for the wall is taken as $\delta_w = 0.04$. As could have been anticipated from the information for harmonically excited systems presented in Fig. 4.6, the effect of wall flexibility is to reduce the effective damping of the system and increase the amplification factor of response, the latter increase being most pronounced in the practically important period range of 0.1 to 0.5 sec.

In Fig. 4.9, the average value of the amplification factor for base wall-shear within the period range T_{11} from 0.1 to 0.5 sec is plotted as a function of the wall flexibility factor d_w for four values of

H/R. The same information is also displayed in Fig. 4.10, with the corresponding value of the maximum base shear normalized with respect to the common factor $m\ddot{X}_g$. Except for the expected differences in the levels of amplification factor and the associated response (note that the absolute maximum value of the average amplification factor in this case is only 2.5), the interrelationship and general trends of these plots are impressively similar to those for the harmonically excited systems considered in Figs. 4.6 and 4.7. Specifically, for systems represented by points in Fig. 4.10 to the right of the heavy dots, the effect of wall flexibility is to reduce the response below the level applicable to rigid tanks. Only for very slender systems with moderate wall flexibility is the response of flexible tanks, like that of liquid-containing tanks, likely to be higher than for the corresponding rigid tanks. It should be noted, however, that the maximum response of solid-containing rigid tanks is generally significantly higher than that of tanks containing a liquid of the same mass density. This matter is addressed further in a later section.

4.4 Relative Effects of Normal and Shearing Stresses

For the bonded medium-wall interface considered, the base shear in the tank wall is contributed partly by normal and partly by circumferential stresses. In Fig. 4.11, the maximum value of the base wall-shear contributed by the normal stresses, $(Q_b^\sigma)_{max}$, is plotted as a fraction of the corresponding total shear, $(Q_b)_{max}$. The results, which are again for the El Centro ground motion record, are plotted as a function of the fundamental period T_{11} of the system under consideration. Three values of H/R in the range between 0.3 and 3.0 and two values of the wall flexibility factor are examined. For rigid tanks ($d_w = 0$), similar plots were presented in Part A. It is observed that within the range of parameters considered, approximately 75 percent of the total base shear in the wall is contributed by the normal pressures.

4.5 Contribution of Higher Modes of Vibration

It has been shown (Veletsos and Younan, 1997) that satisfactory approximations to the critical responses of rigid tanks are obtained by considering in the governing series expressions only the terms associated with the fundamental vertical mode of vibration of the contained medium. It should be recalled that the contributions of all horizontal modes of vibration are duly provided for in the method of analysis. For the flexible tanks examined here, it can similarly be shown that the dominant contributor to each response quantity is the term associated with the fundamental mode of vibration of the tank-medium system. This is demonstrated in Fig. 4.12 in which the exact values of the maximum base shear induced by the El Centro ground motion record are compared with those computed considering only the first term in the series. The results are plotted against the fundamental natural period of the system T_{11} for three values of the flexibility factor d_w. It is observed that the agreement between the two solution sets is indeed excellent for all practical purposes. It should be added, however, that the assumption of shear-beam action for the tank wall which underlies the method of analysis is not expected to be as appropriate for tall tanks as for broad tanks.

4.6 Overturning Base Moment

Considering that the response of the system is dominated by the contribution of the fundamental mode of vibration and that the dynamic wall pressures for this mode increase approximately as a quarter-sine from zero at the base to a maximum at the top, and further recalling that the height to the centroid of this distribution is $h = (2/\pi)H$, the maximum overturning moment across a section immediately above the base may be taken as the product of the corresponding base shear and this value of h. For systems with H/R = 1 subjected to the El Centro ground motion, the exact values of h are shown in Fig. 4.13.

4.7 Effect of Wall Inertia

In the numerical solutions presented so far, the wall mass was presumed to be negligible compared to the participating mass of the retained medium. While the effect of the wall inertia may be evaluated exactly from expressions presented in previous sections, the following simple, approximate procedure would be adequate for all practical purposes.

The maximum base shear in the wall of a tank with mass, $(Q_b)_{max}^{m_w}$, may be related to that of the massless wall, $(Q_b)_{max}$, by

$$(Q_b)_{max}^{m_w} = (Q_b)_{max} + m_o \ddot{X}_g (AF) \tag{24}$$

where m_o = the effective mass of the tank wall; and the amplification factor AF may be taken equal to that for the massless tank. The value of m_o normalized with respect to the total mass of the tank wall, m_w, is plotted as a function of the wall flexibility factor d_w in Fig. 4.14. For rigid tanks, the ratio is naturally unity, but for flexible tanks, particularly for the more compliant systems with large values of H/R and d_w, it may be substantially smaller. For the computation of the effect of the wall inertia on the overturning base moment, the effective height h may be taken equal to that for the massless tank..

Table 4.1: Static Values of Top Radial Pressure $\sigma_{st}(1)$, Base Shear $(Q_b)_{st}$, and of Effective height h; Systems with massless walls and $\nu = 1/3$.

H/R	$d_w = 0$	$d_w = 0.5$	$d_w = 1$	$d_w = 1.5$	$d_w = 2$	$d_w = 3$
(1)	(2)	(3)	(4)	(5)	(6)	(7)
			(a) Values of $-\sigma_{st}(1)/\rho\ddot{X}_g R$			
0.30	0.366	0.293	0.245	0.210	0.183	0.146
0.50	0.541	0.398	0.315	0.260	0.222	0.170
0.80	0.672	0.466	0.356	0.288	0.241	0.182
1.00	0.710	0.483	0.365	0.294	0.246	0.185
1.25	0.732	0.492	0.370	0.297	0.247	0.186
1.50	0.742	0.495	0.372	0.298	0.248	0.186
1.75	0.746	0.496	0.372	0.298	0.248	0.186
2.00	0.748	0.497	0.373	0.298	0.248	0.186
2.50	0.749	0.497	0.372	0.298	0.248	0.186
3.00	0.749	0.497	0.372	0.298	0.248	0.186
			(b) Values of $-(Q_b)_{st}/m\ddot{X}_g$			
0.30	0.392	0.320	0.272	0.236	0.209	0.170
0.50	0.567	0.430	0.348	0.293	0.253	0.199
0.80	0.715	0.513	0.402	0.331	0.282	0.217
1.00	0.771	0.543	0.421	0.345	0.292	0.224
1.25	0.816	0.567	0.436	0.355	0.300	0.229
1.50	0.847	0.583	0.447	0.362	0.305	0.232
1.75	0.869	0.594	0.454	0.367	0.309	0.234
2.00	0.885	0.603	0.459	0.371	0.312	0.236
2.50	0.908	0.615	0.467	0.376	0.315	0.238
3.00	0.923	0.623	0.472	0.380	0.318	0.240
			(c) Values of h/H			
0.30	0.595	0.589	0.584	0.580	0.576	0.570
0.50	0.590	0.582	0.575	0.570	0.565	0.558
0.80	0.580	0.570	0.562	0.557	0.552	0.546
1.00	0.573	0.562	0.555	0.550	0.546	0.539
1.25	0.565	0.555	0.548	0.543	0.539	0.534
1.50	0.558	0.548	0.542	0.538	0.534	0.529
1.75	0.552	0.543	0.537	0.533	0.530	0.526
2.00	0.547	0.539	0.534	0.530	0.527	0.523
2.50	0.540	0.533	0.528	0.525	0.523	0.519
3.00	0.534	0.528	0.524	0.521	0.519	0.517

Table 4.2: Fundamental Natural Period T_{11} of Solid-Containing Tanks; Systems with massless walls and $\nu = 1/3$.

H/R	$d_w = 0$	$d_w = 0.5$	$d_w = 1$	$d_w = 1.5$	$d_w = 2$	$d_w = 3$
(1)	(2)	(3)	(4)	(5)	(6)	(7)
			Values of T_{11}/T_1			
0	1.0	1.0	1.0	1.0	1.0	1.0
0.30	0.841	0.857	0.872	0.884	0.895	0.912
0.50	0.682	0.746	0.794	0.828	0.853	0.886
0.80	0.504	0.660	0.746	0.798	0.832	0.874
1.00	0.423	0.633	0.733	0.790	0.827	0.871
1.25	0.350	0.614	0.724	0.785	0.823	0.870
1.50	0.297	0.603	0.719	0.782	0.821	0.868
1.75	0.258	0.596	0.716	0.780	0.820	0.868
2.00	0.227	0.592	0.714	0.779	0.819	0.867
2.50	0.184	0.587	0.711	0.777	0.818	0.867
3.00	0.154	0.584	0.710	0.776	0.818	0.867

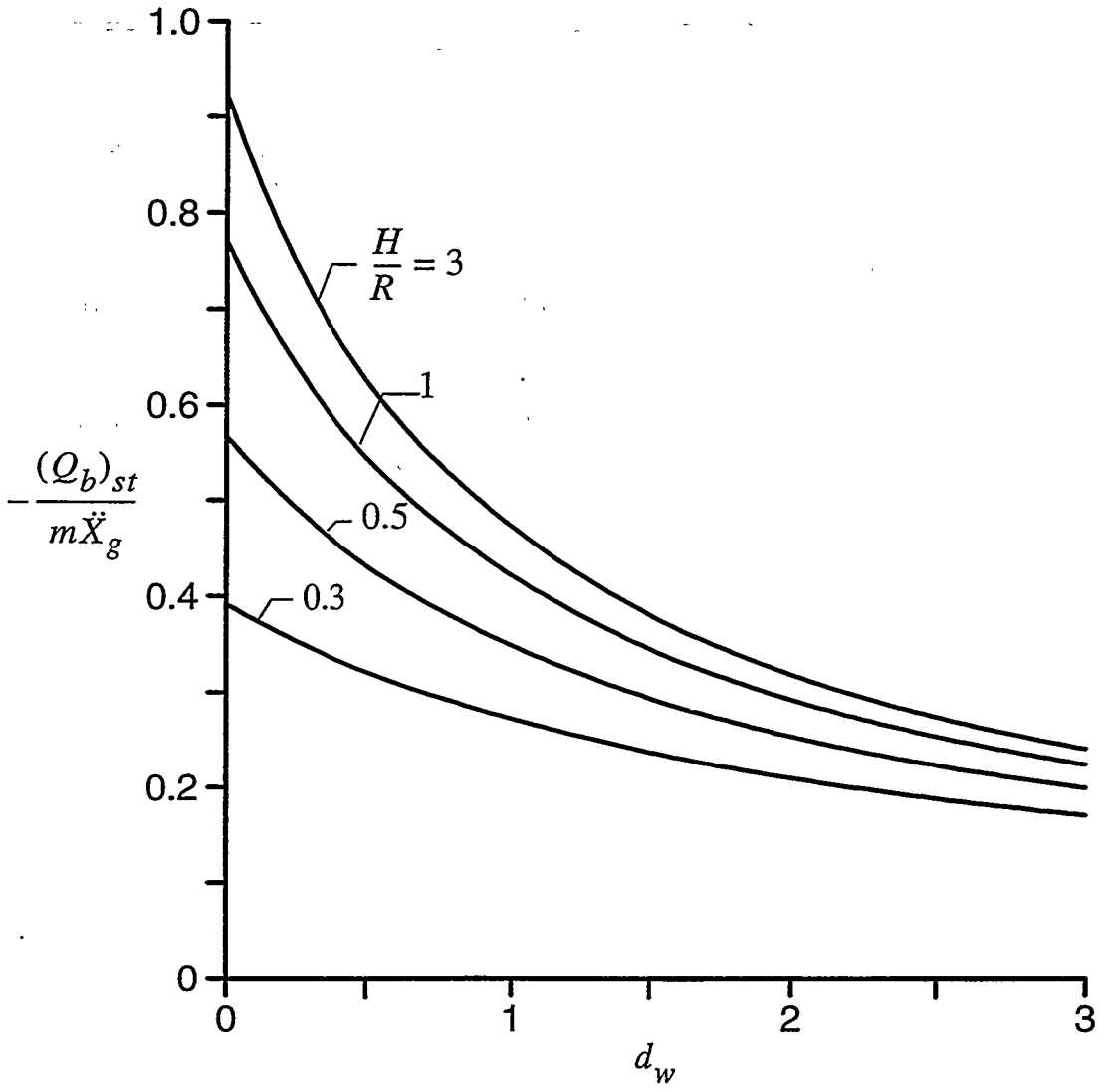

Figure 4.1 Normalized Values of Base Shear for Statically Excited Systems with Different Wall Flexibilities and Slenderness Ratios; $m_w = 0$ and $\nu = 1/3$.

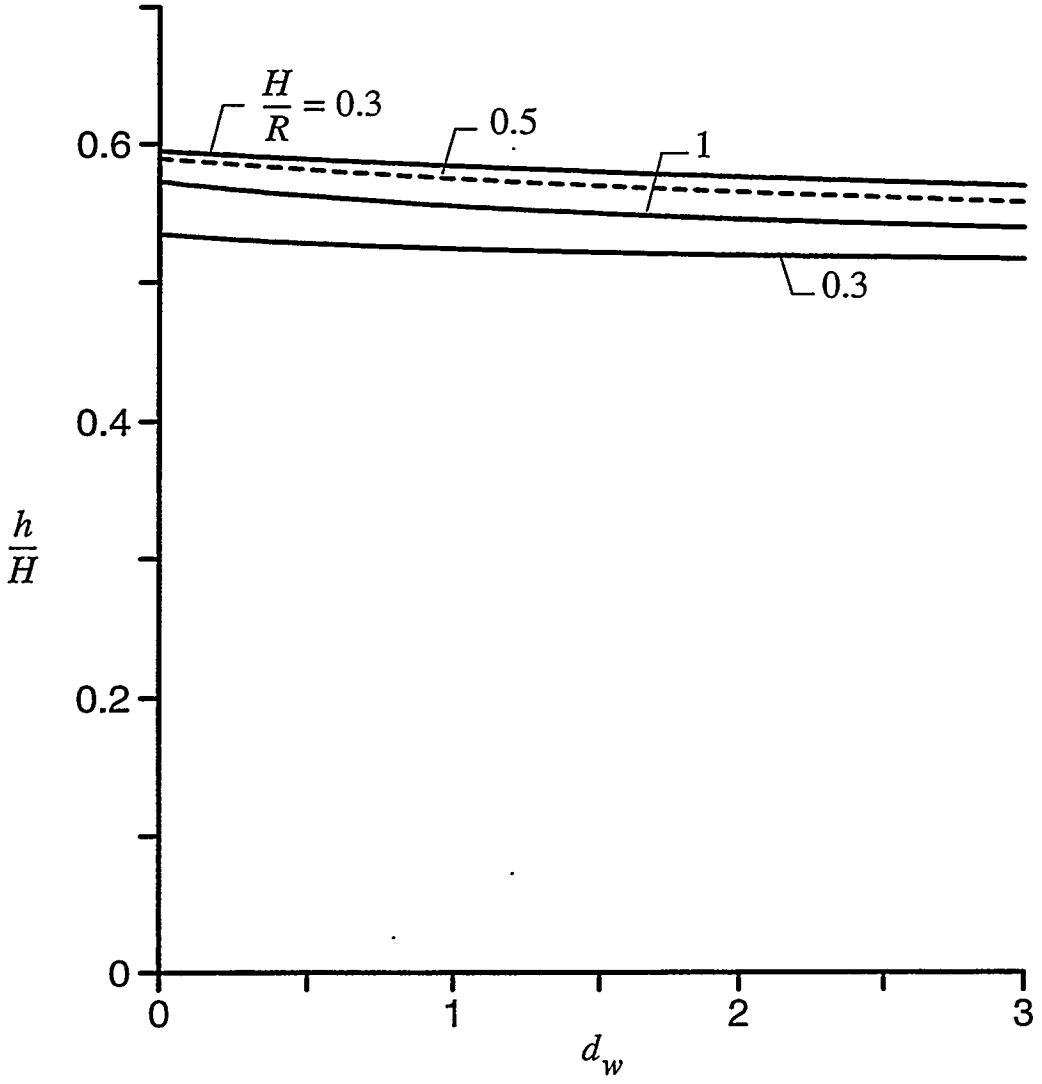

Figure 4.2 Normalized Values of Effective Height for Statically Excited Systems with Different Wall Flexibilities and Slenderness Ratios; $m_w = 0$ and $\nu = 1/3$.

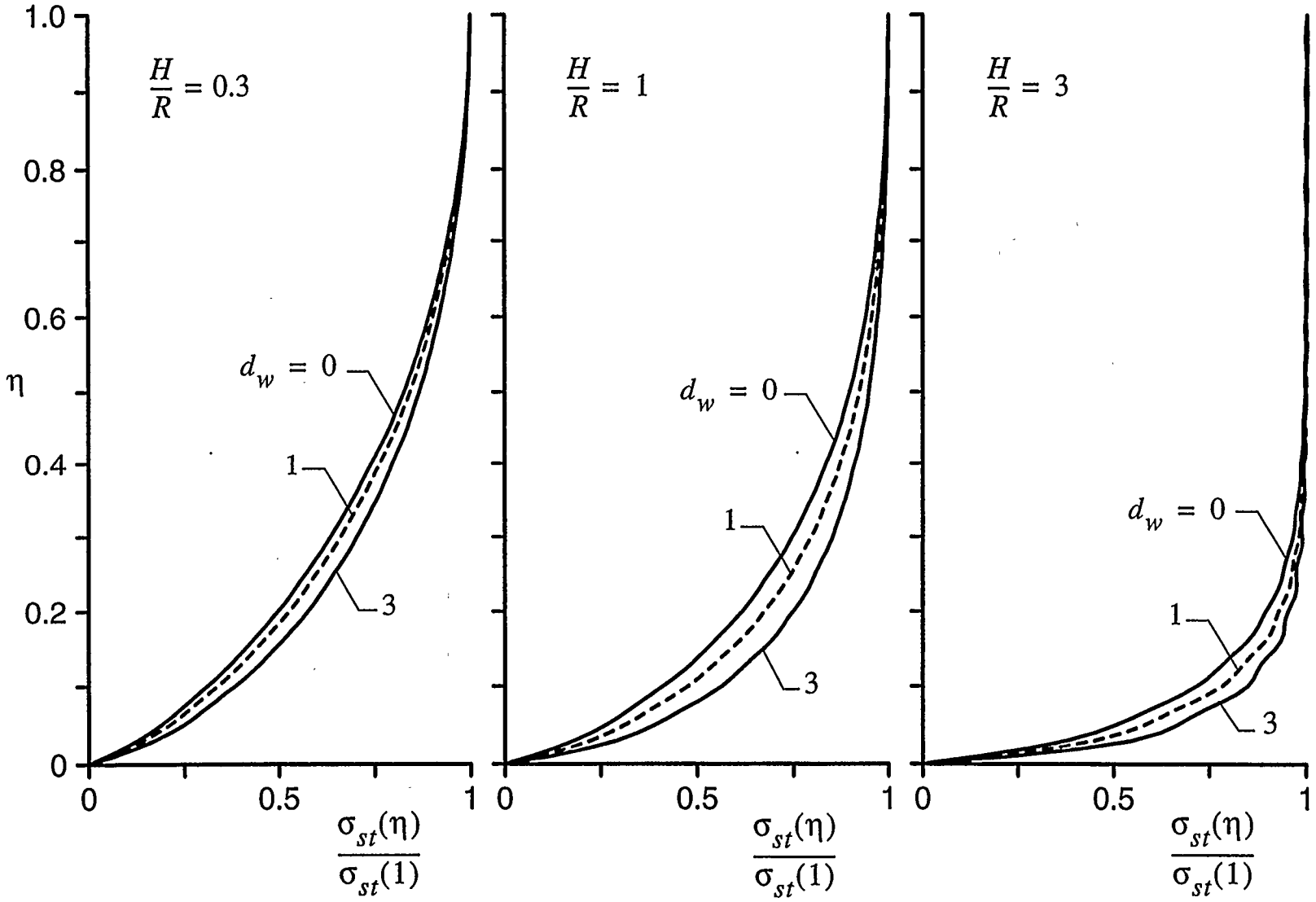

Figure 4.3 Heightwise Variations of Static Values of Normal Wall Pressures Induced in Tanks of Different Flexibilities and Slenderness Ratios; $m_w = 0$ and $\nu = 1/3$.

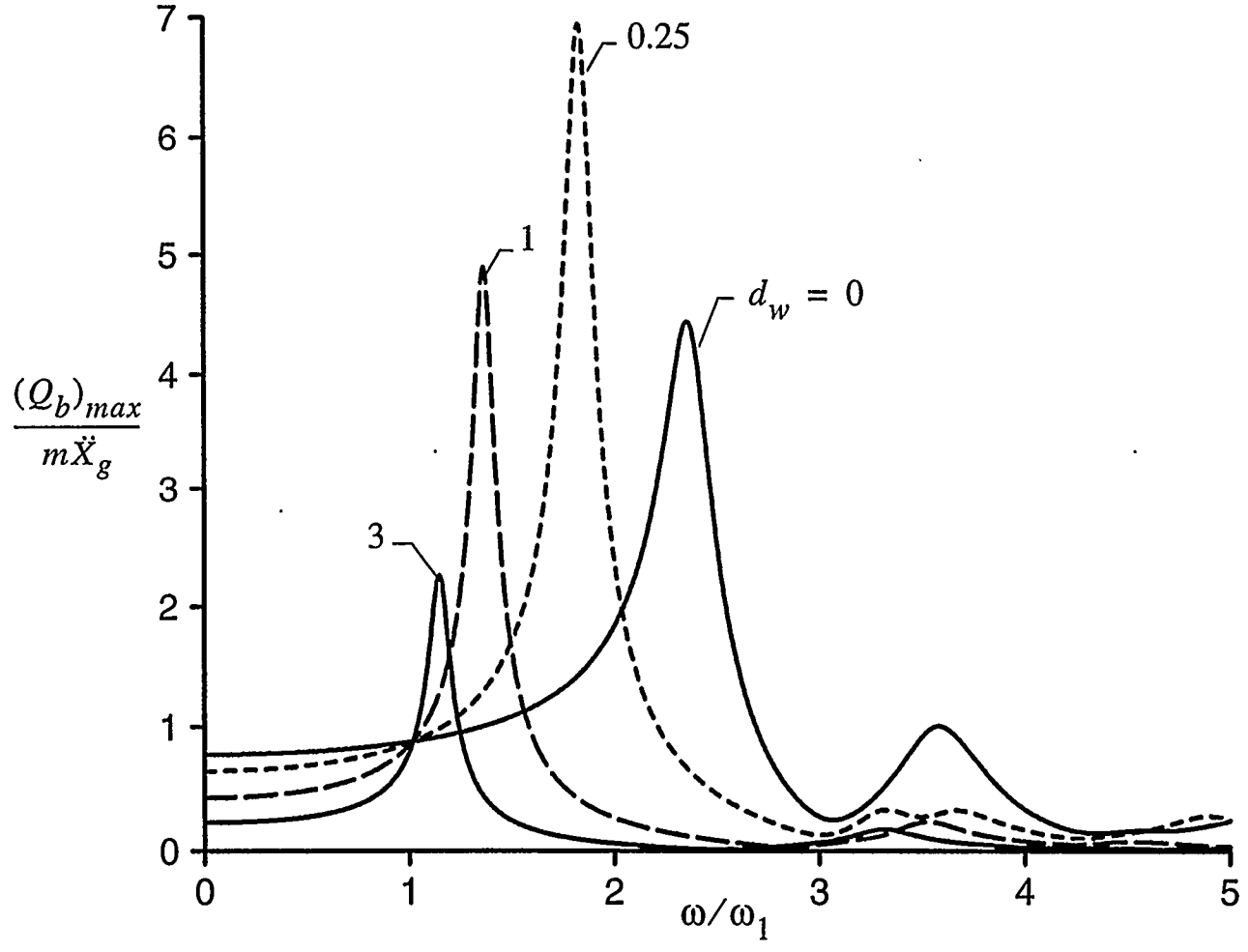

Figure 4.4 Frequency Response Curves for Base Shear in Wall of Harmonically Excited Tanks with Different Wall Flexibilities; H/R = 1, $m_w = 0$, $\delta_w = 0.04$, $\nu = 1/3$ and $\delta = 0.1$

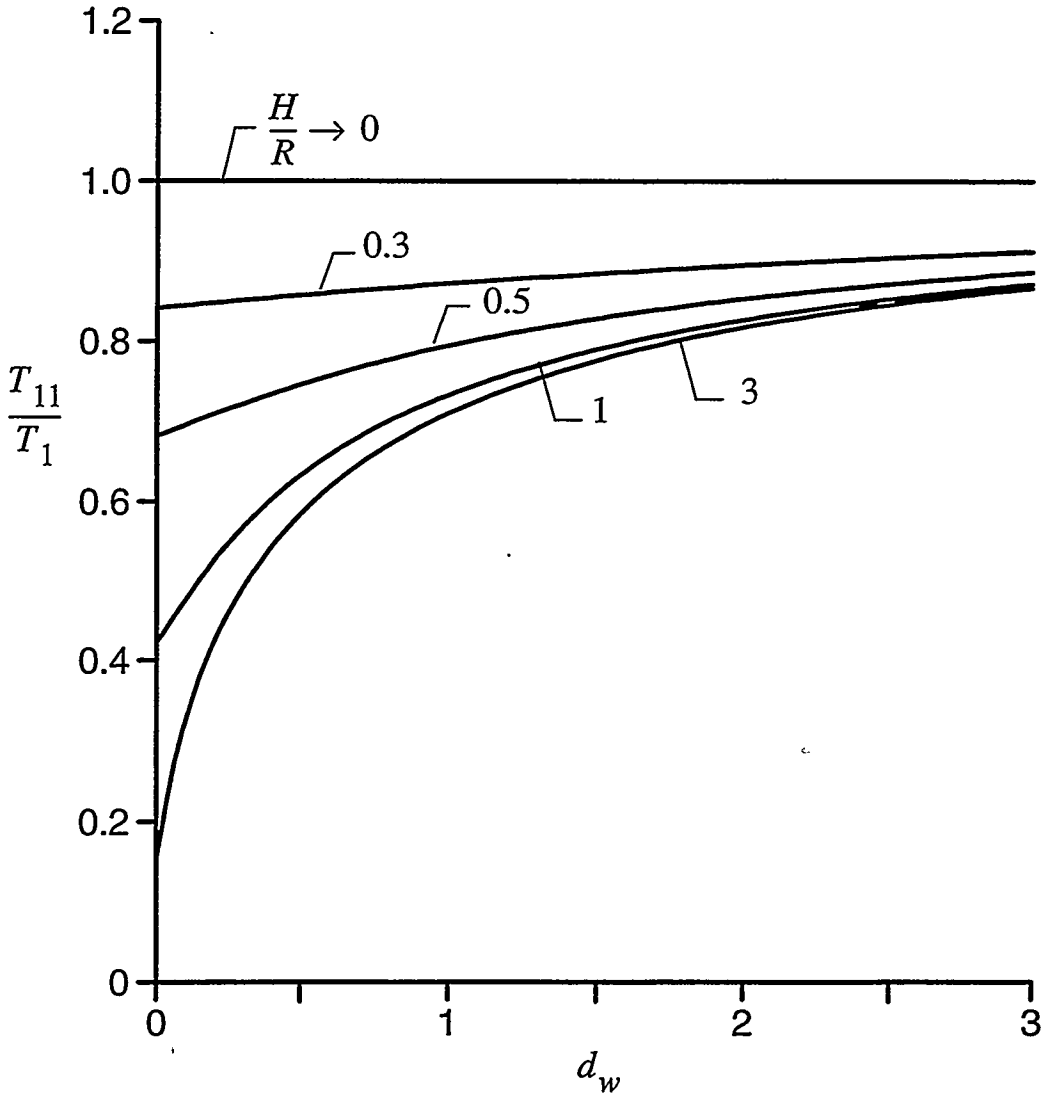

Figure 4.5 Fundamental Natural Period of Tanks of Different Slenderness Ratios and Wall Flexibilities; $m_w = 0$ and $\nu = 1/3$.

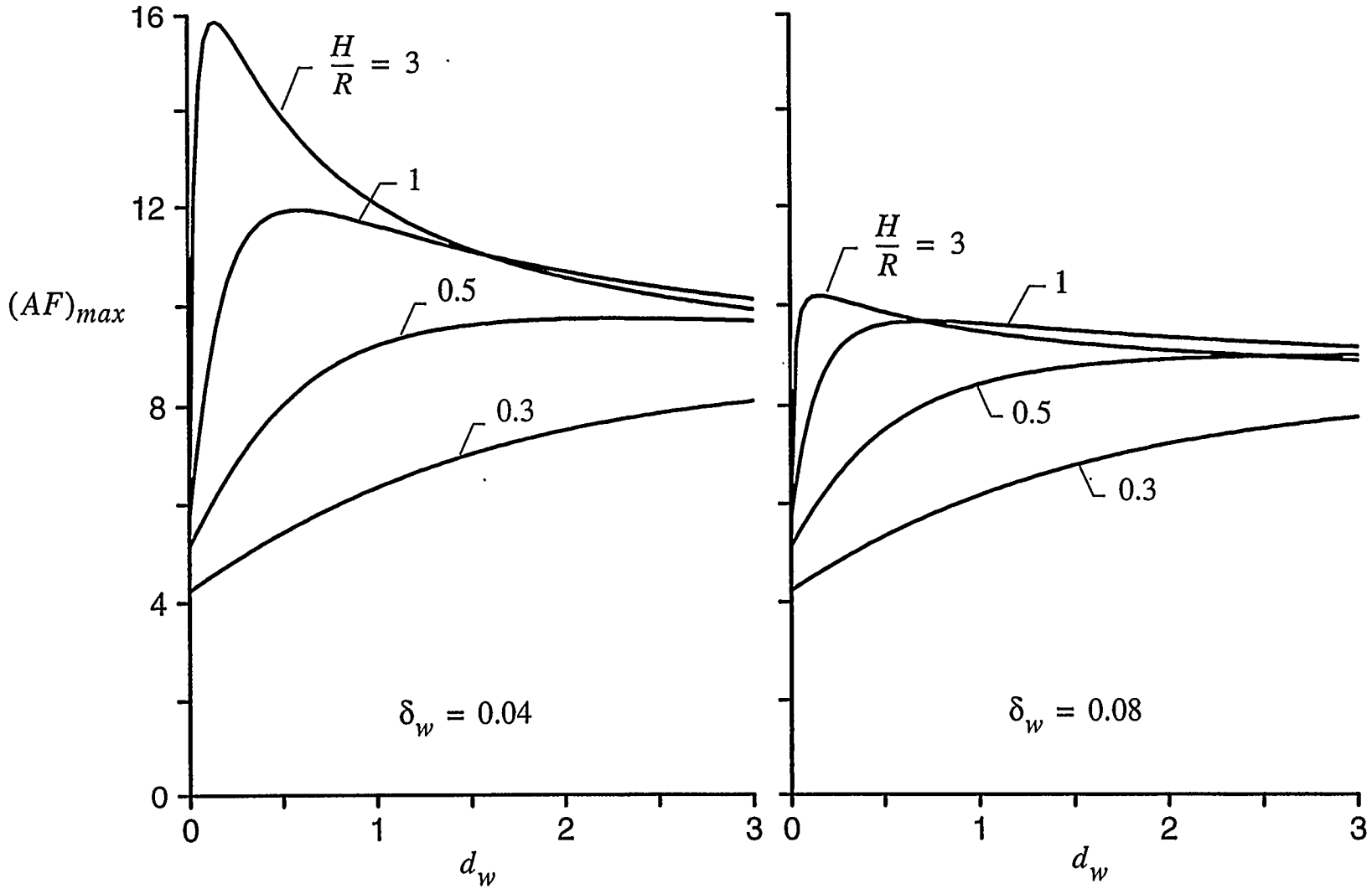

Figure 4.6 Maximum Amplification Factors for Base Shear in Wall of Harmonically Excited Tanks with Different Slenderness Ratios and Wall Flexibilities; $m_w = 0$, $\delta_w = 0.04$ & 0.08, $\nu = 1/3$ and $\delta = 0.1$.

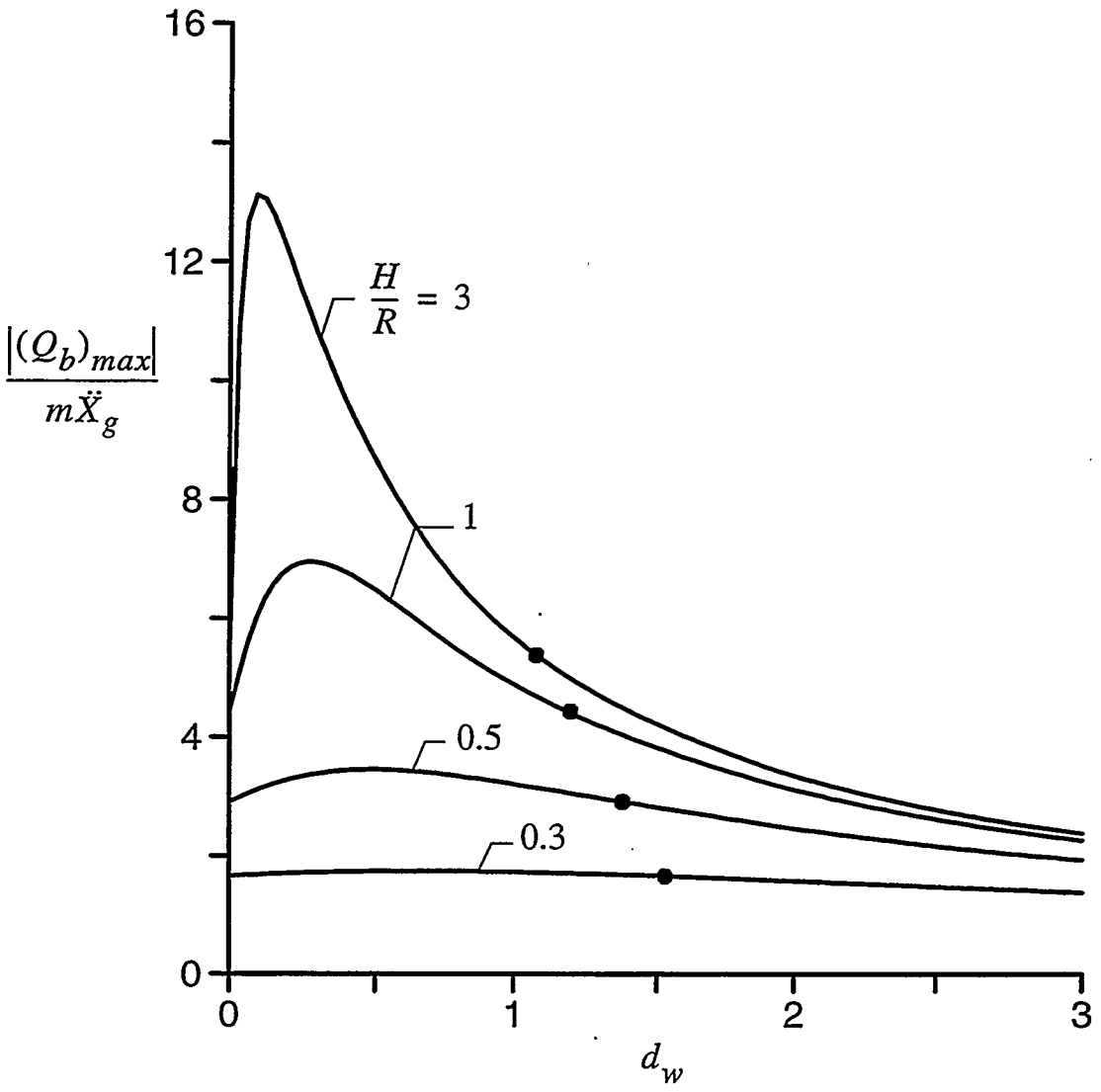

Figure 4.7 Normalized Values of Absolute Maximum Base Shear in Wall of Harmonically Excited Tanks with Different Slenderness Ratios and Wall Flexibilities; $m_w = 0$, $\delta_w = 0.04$, $\nu = 1/3$ and $\delta = 0.1$

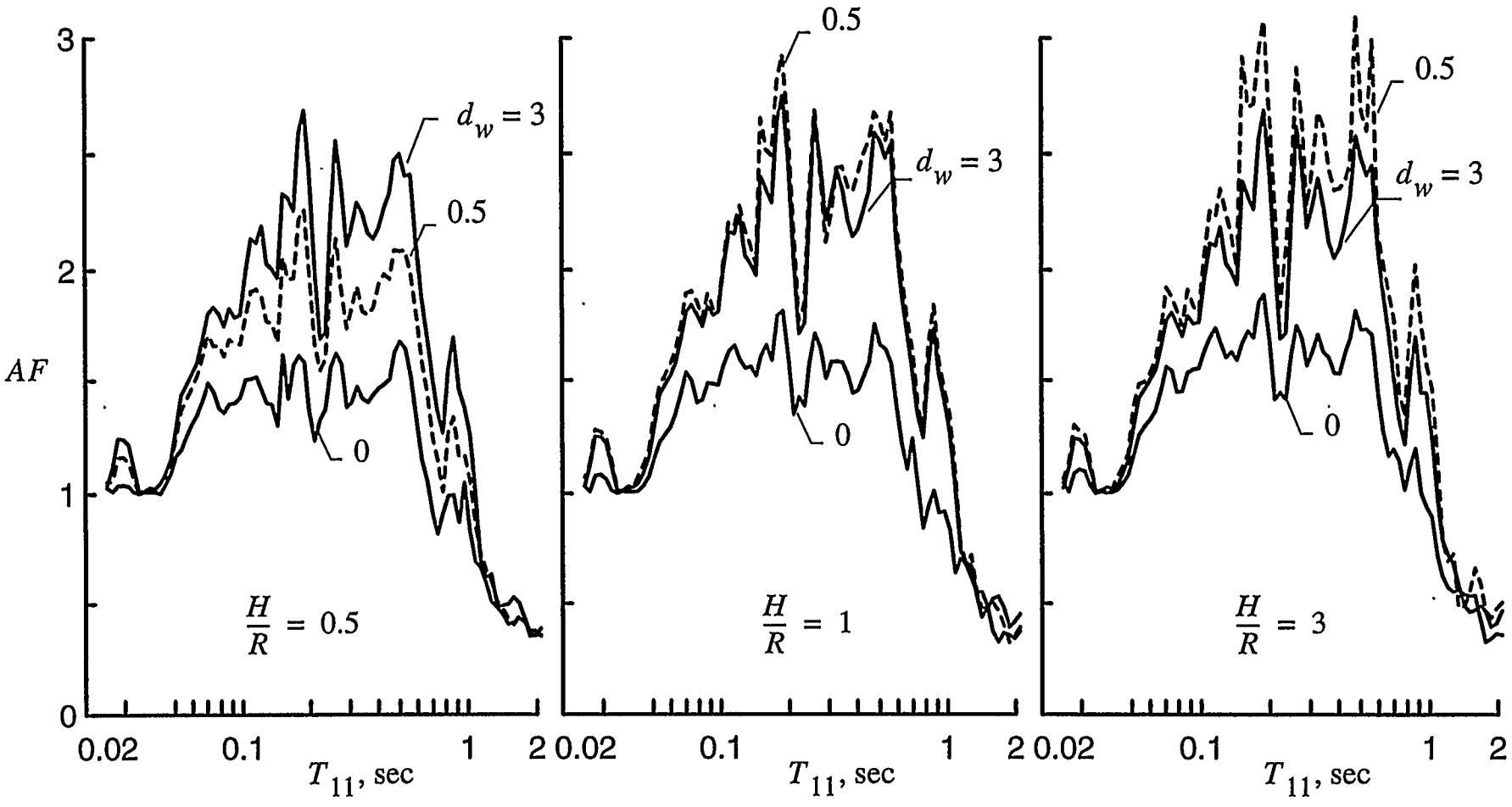

Figure 4.8 Amplification Factors for Base Shear in Wall of Tanks with Different Slenderness Ratios and Wall Flexibilities Subjected to El Centro Record; $m_w = 0$, $\delta_w = 0$, $\nu = 1/3$ and $\delta = 0.1$.

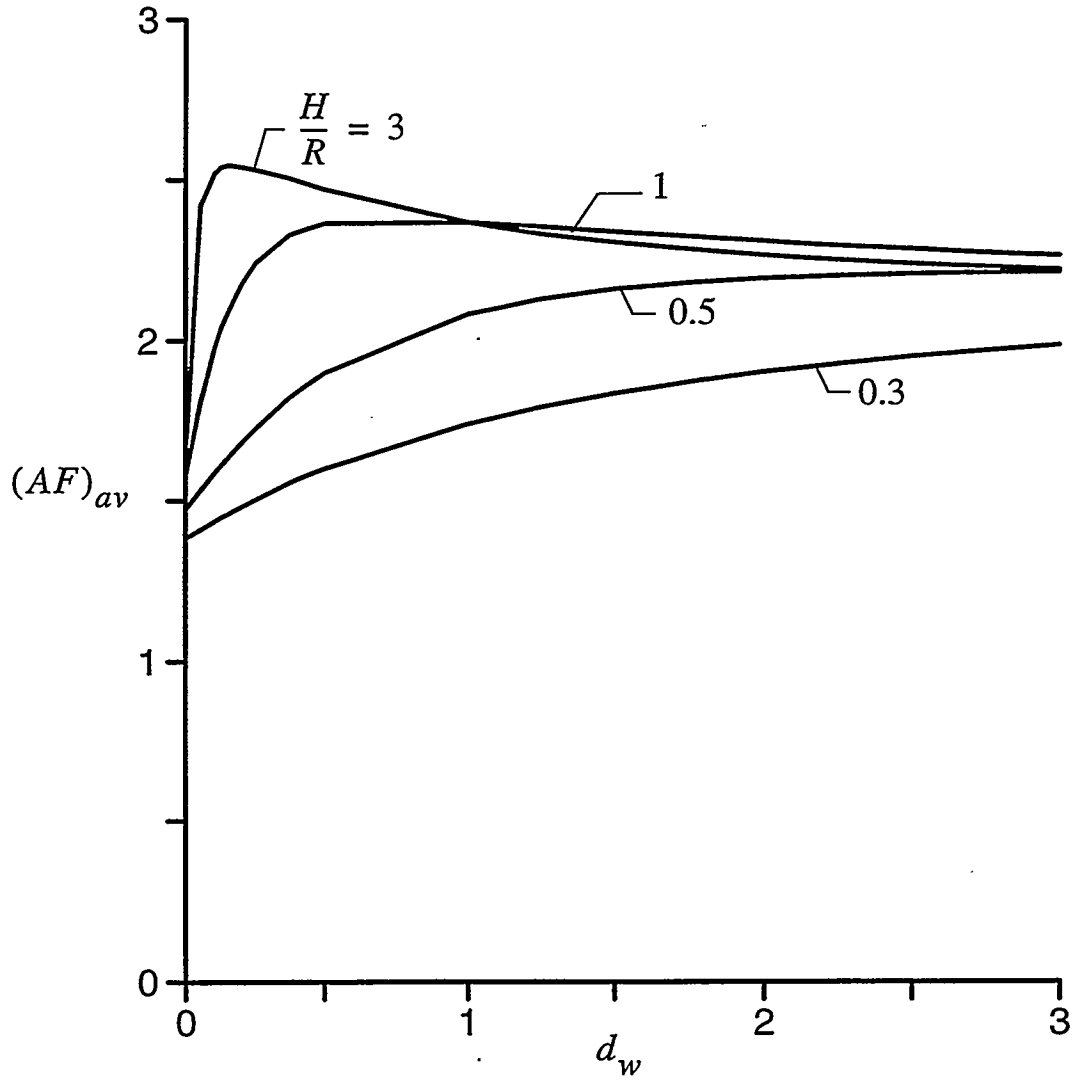

Figure 4.9 Average Amplification Factors for Base Shear in Wall of Tanks with Different Slenderness Ratios and Wall Flexibilities Subjected to El Centro Record; $m_w = 0$, $\delta_w = 0.04$, $\nu = 1/3$ and $\delta = 0.1$; AF averaged over period range $T_{11} = 0.1$ to 0.5 sec.

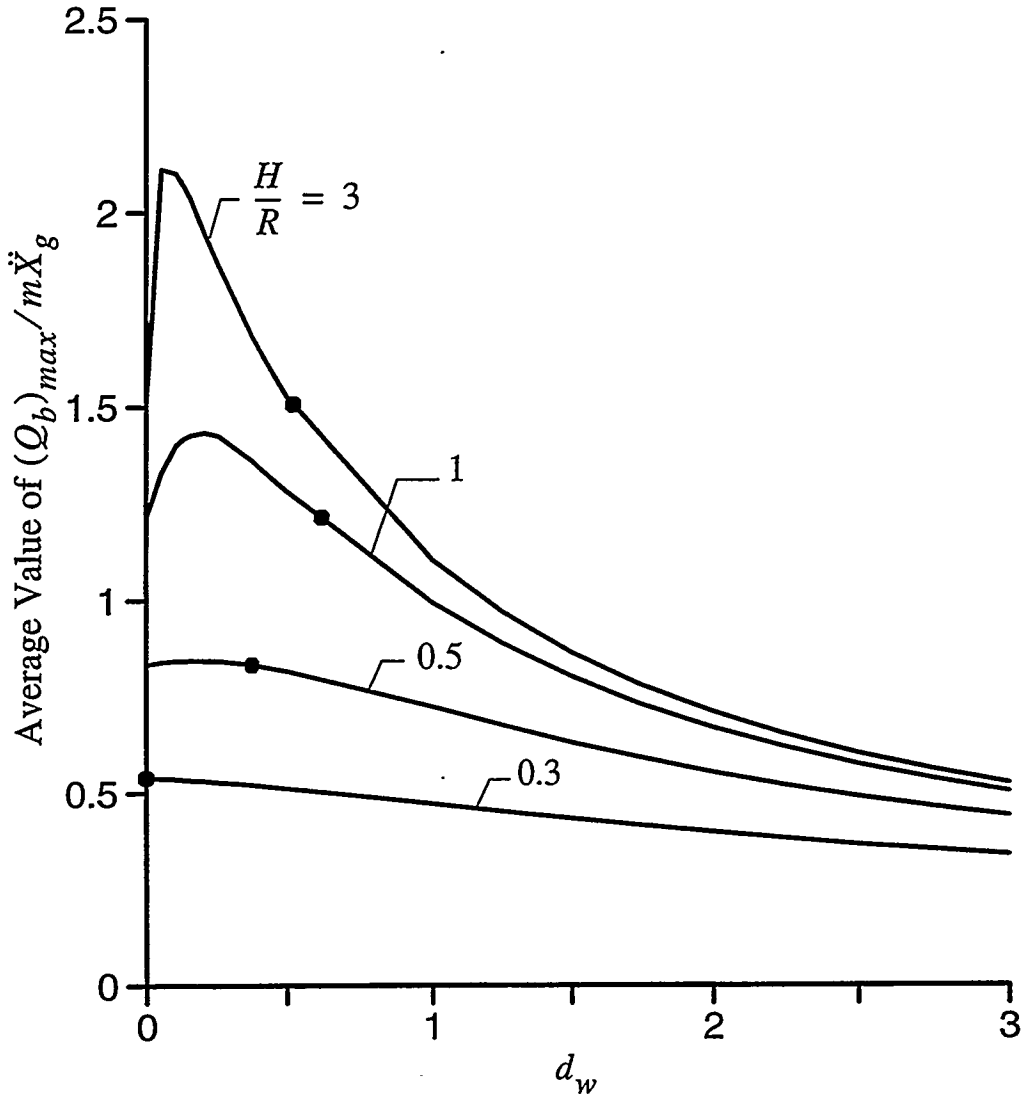

Figure 4.10 Average Value of Maximum Base Shear in Wall of Tanks with Different Slenderness Ratios and Wall Flexibilities Subjected to El Centro Record; $m_w = 0$, $\delta_w = 0$, $\nu = 1/3$ and $\delta = 0.1$; base shear averaged over period range $T_{11} = 0.1$ to 0.5 sec.

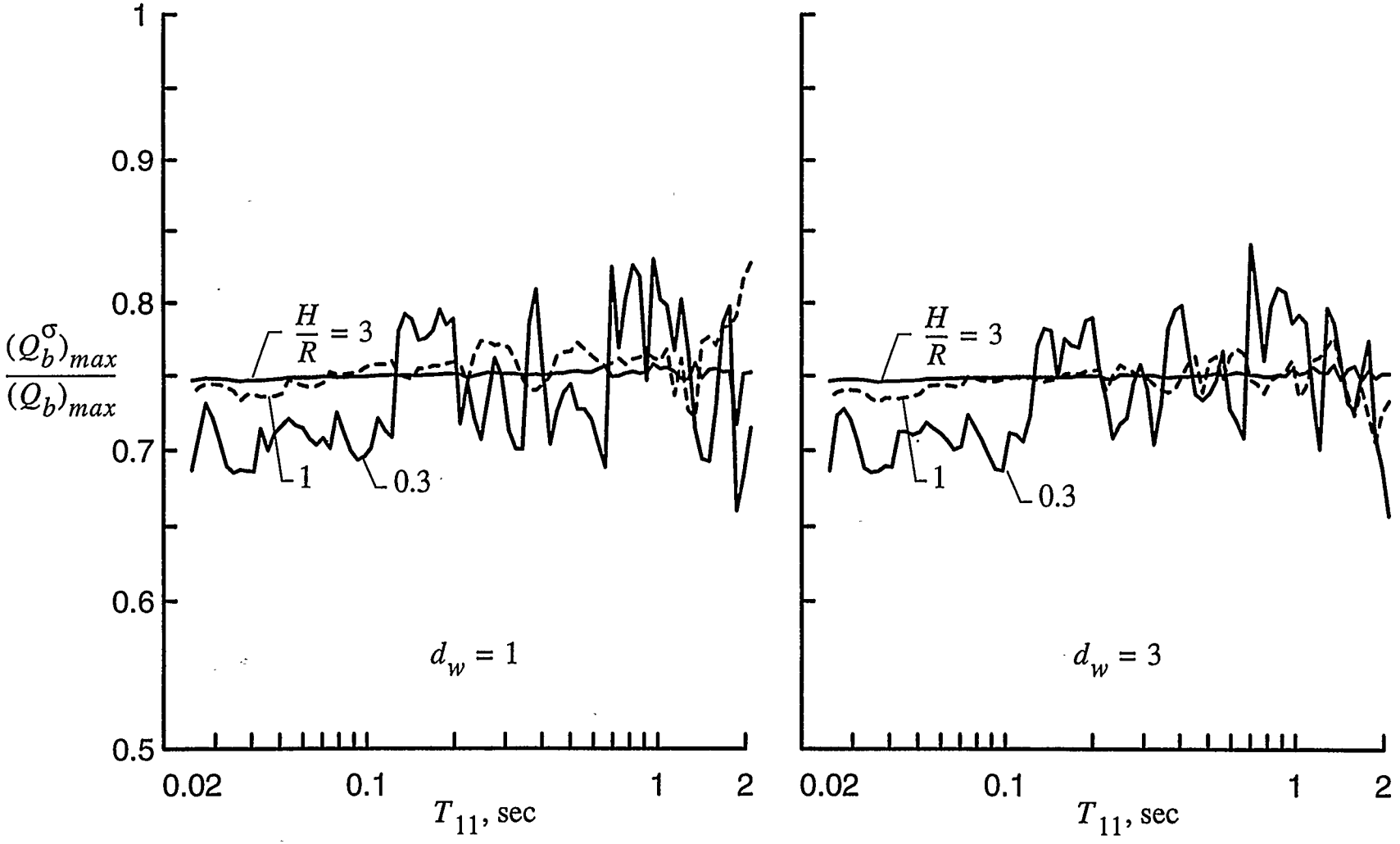

Figure 4.11 Portion of Total Base Shear Induced by Normal Wall Pressures in Tanks Subjected to El Centro Record; $m_w = 0$, $\delta_\omega = 0$, $\nu = 1/3$ and $\delta = 0.1$.

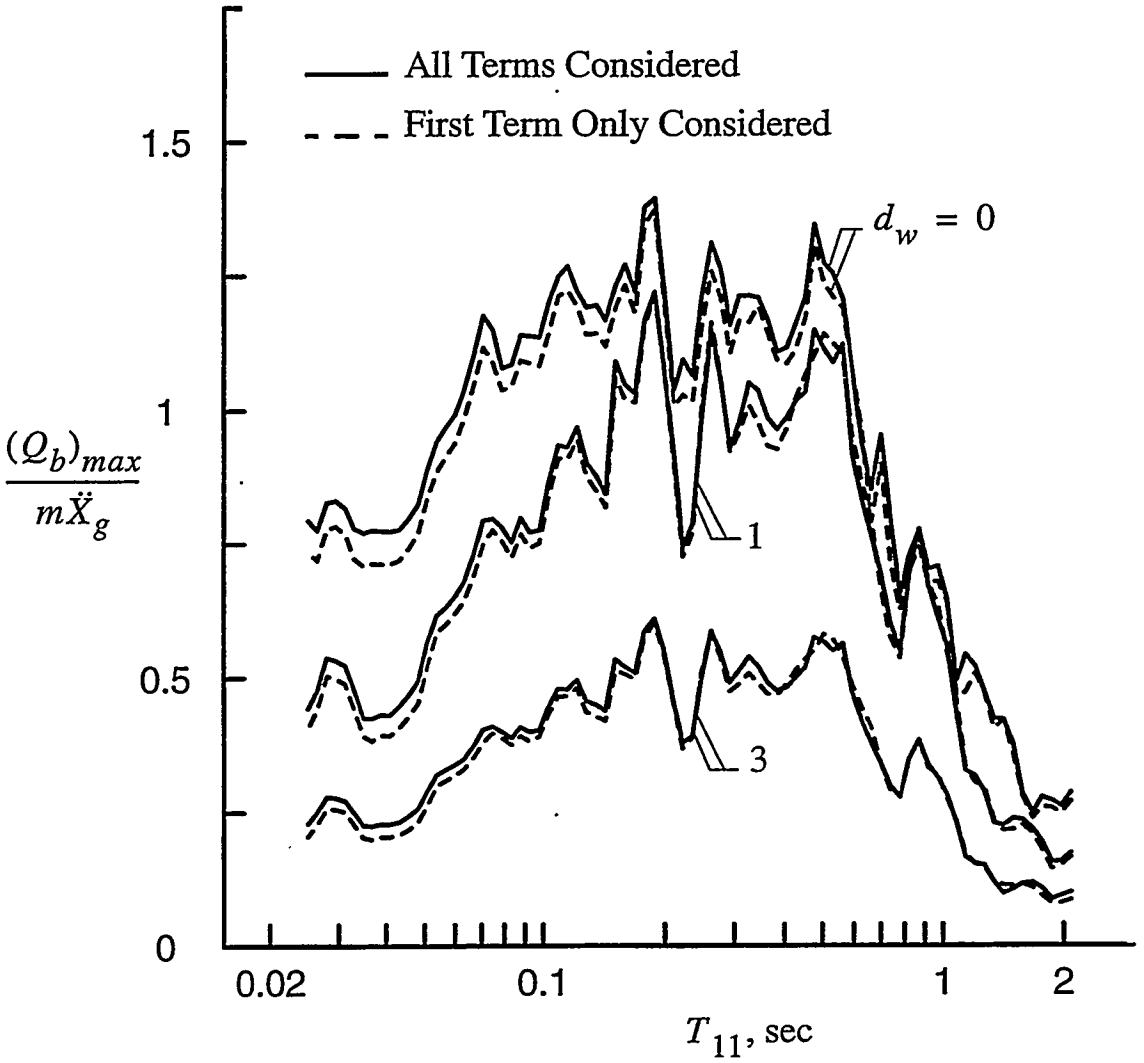

Figure 4.12 Maximum Values of Base Shear in Wall of Tanks with Different Flexibilities Computed Using One and Many Vertical Modes of Vibration; Systems with H/R = 1, $m_w = 0$, $\delta_w = 0$, $\nu = 1/3$ and $\delta = 0.1$ subjected to El Centro Record.

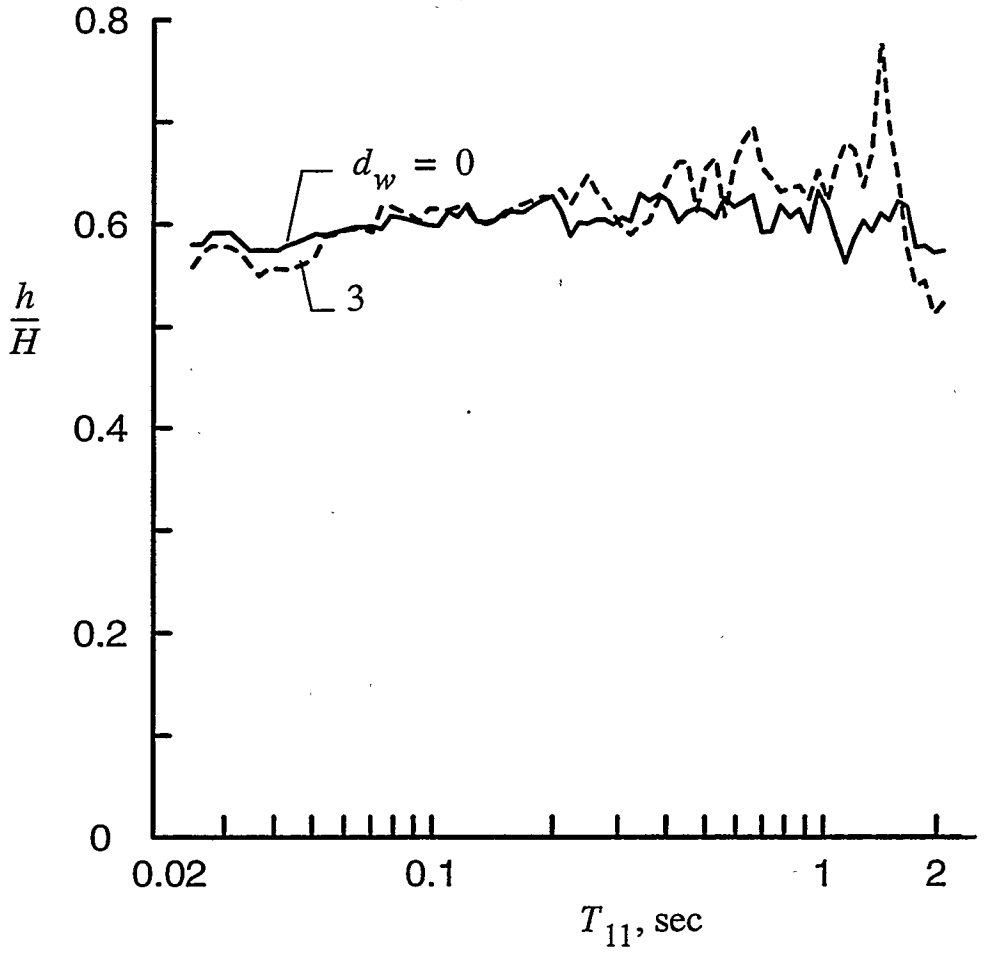

Figure 4.13 Normalized Effective Heights of Tanks of Different Wall Flexibilities Subjected to El Centro Record; H/R = 1, $m_w = 0$, $\delta_w = 0$, $\nu = 1/3$ and $\delta = 0.1$.

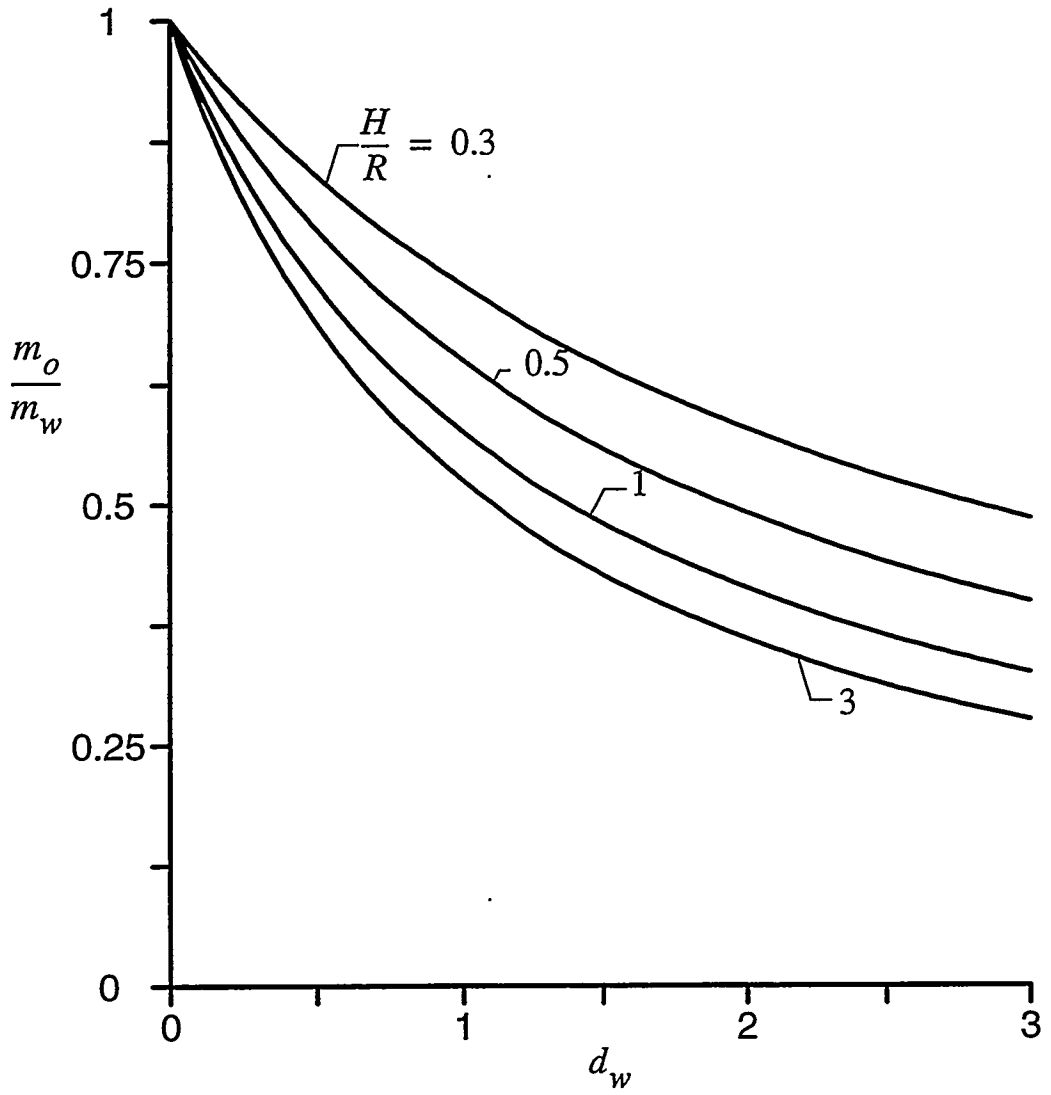

Figure 4.14 Effective Wall Mass for Statically Excited Tanks of Different Slenderness Ratios and Wall Flexibilities; $\delta_w = 0$, $\nu = 1/3$ and $\delta = 0.1$.

SECTION 5

FOUNDATION FORCES

As for rigid tanks, the maximum shearing force transmitted to the foundation of a flexible tank, $\tilde{Q}$, and the corresponding moment, $\tilde{M}$, can most effectively be computed from the inertial forces acting on the tank and the contained material. To a reasonable degree of approximation, these forces may be expressed as

$$\tilde{Q}_{max} = -(m + m_w)\ddot{X}_g(AF) \tag{25}$$

$$\tilde{M}_{max} = -\frac{1}{2}(m + m_w)\ddot{X}_g H(AF) \tag{26}$$

where the amplification factor *AF* may be taken equal to that reported for the base shear in the tank wall. More precise expressions may be determined by evaluating the integrals defined by equations (54) and (55) of Part A and superimposing the effects of the wall inertia forces defined by (22b) and (23b).

SECTION 6

INTERRELATIONSHIP OF RESPONSES OF SOLID- AND LIQUID-CONTAINING TANKS

In assessing the interrelationship of the responses of tanks containing a solid or a liquid, it is important that the following properties of the two materials be kept in mind:

1. Possessing no shearing resistance, an inviscid liquid transmits its horizontal inertia forces directly to the wall. By contrast, a portion of the inertia forces for a solid-containing tank is transmitted by horizontal shearing action to the base.
2. With the liquid being for all practical purposes incompressible, the impulsive component of the liquid mass acts as if it were rigidly attracted to the tank wall and experiences the same motion as the wall. By contrast, a solid acts as a multi-degree-of-freedom elastic medium with its own natural frequencies and modes, and, depending on the relationship of its properties and the characteristics of the forcing function, it may amplify or deamplify the wall motion.
3. In a tank for which the upper surface of the contained liquid is rigidly capped, the entire mass of the liquid acts impulsively as a rigidly attached body. However, for a liquid with a free upper surface, only a fraction of the contained mass acts impulsively; the remaining part, known as the convective component, experiences rocking or sloshing motions. The convective component may be quite substantial for broad, shallow tanks. There is, of course, no counterpart of this convective or sloshing action in a solid-containing tank.

For a liquid-containing **rigid** tank, the instantaneous value of the total wall force or base shear, $Q_b^r(t)$, may be expressed as

$$Q_b^r(t) = m_i \ddot{x}_g(t) + \sum_{n=1}^{\infty} m_{cn} A_{cn}(t) \tag{27}$$

where m_i = the impulsive component of the contained mass, m_{cn} = the *n*th convective component, and $A_{cn}(t)$ = the instantaneous pseudoacceleration of the latter component. The sum of m_i and all m_{cn} is equal to the total liquid mass m.

For representative earthquake ground motions and for tanks of the proportions normally encountered in practice, the maximum values of the pseudoacceleration $A_{cn}(t)$ are substantially smaller than the maximum ground acceleration $\ddot{X}_g$, with the result that the contribution of the convective components is for most practical purposes negligible. Within the bounds of this approximation, the maximum val-

ues of the base shear for rigid tanks containing either a solid or liquid may be expressed as

$$(Q_b)_{max} = m_e \ddot{X}_g (AF) \tag{28}$$

where m_e = the effective mass of the contained material (m_i for a liquid-containing tank), and *AF* = an appropriate amplification or deamplification factor.

The values of m_e normalized with respect to the total contained mass *m* are plotted in Fig. 6.1 as a function of the slenderness ratio *H/R* for both liquid- and solid-containing tanks. The elastic solid in these solutions is presumed to be bonded to the base and the tank wall, and its Poisson's ratio $\nu = 1/3$. It is observed that the effective mass of a solid-containing tank is larger than that of the same tank containing a liquid of the same total mass. Considering that a portion of the inertia forces for the solid gets transferred by horizontal shearing action to the base and that a liquid does not possess such capacity, the larger effective mass for the solid-containing system may be surprising. It must be recalled, however, that only the impulsive component of the liquid mass is considered in this comparison and that there is no counterpart of the convective or sloshing component for a solid.

The normal and circumferential stresses induced by the solid on the wall increase from the base to the top as indicated in Fig. 4.3, while the impulsive normal pressures induced by the liquid increase from zero at the top to a maximum at the base. The normalized values of the height *h* to the centroid of these pressures for the two materials are compared Fig. 6.1. The solid in these like all other solutions presented is presumed to be bonded to the wall.

For an incompressible liquid, the amplification factor *AF* in (28) is unity, whereas for a compressible elastic solid it may have the much larger values identified in Fig. 4.9 of Part A. Considering that the effective mass m_e for a solid-containing system is also greater than for the liquid-containing system, it should be clear that the dynamic wall pressures and associated forces induced by the solid may be substantially larger that those induced by a liquid of the same density. This conclusion, however, is limited to rigid tanks.

For **flexible** tanks, the interrelationship of the critical responses of solid- and liquid-containing systems is considerably more involved, and its precise definition requires further study. However, the following qualitative conclusions may be drawn by assuming, as it is reasonable to do, that (28) also approximates the response of flexible tanks.

For liquid-containing flexible tanks, the effective mass m_e is effectively equal to or only somewhat smaller than that for the corresponding rigid tanks, while the amplification factor AF may be substantially larger than the unit value applicable to rigid tanks. By contrast, for solid-containing flexible tanks, not only is the effective mass significantly smaller than for the corresponding rigid tanks (see Fig. 4.1), but the AF, as demonstrated in Fig. 4.8, is of the same order of magnitude or substantially

higher than for the corresponding rigid tanks. Because of these opposing effects on the values of m_e and *AF,* the critical responses of the solid-containing systems may be higher than, equal to, or lower than those induced in tanks of the same dimensions by liquids of the same density. The following more specific predictions can also be made:

1. For tall, slender tanks with low to moderate wall flexibilities, the effective damping of the retained material in a solid-containing tank is quite low and so is its ability to transmit the resulting inertial forces by horizontal shearing action to the base. The critical responses of such tanks are not likely to be much different from those induced by a liquid of the same mass density.
2. For shallow, broad tanks of moderate to high wall flexibilities, on the other hand, both the effective damping and the shearing resistance of the retained medium in solid-containing tanks are quite high, with the result that the critical responses of such tanks are likely to be smaller than those of the corresponding liquid-containing tanks.

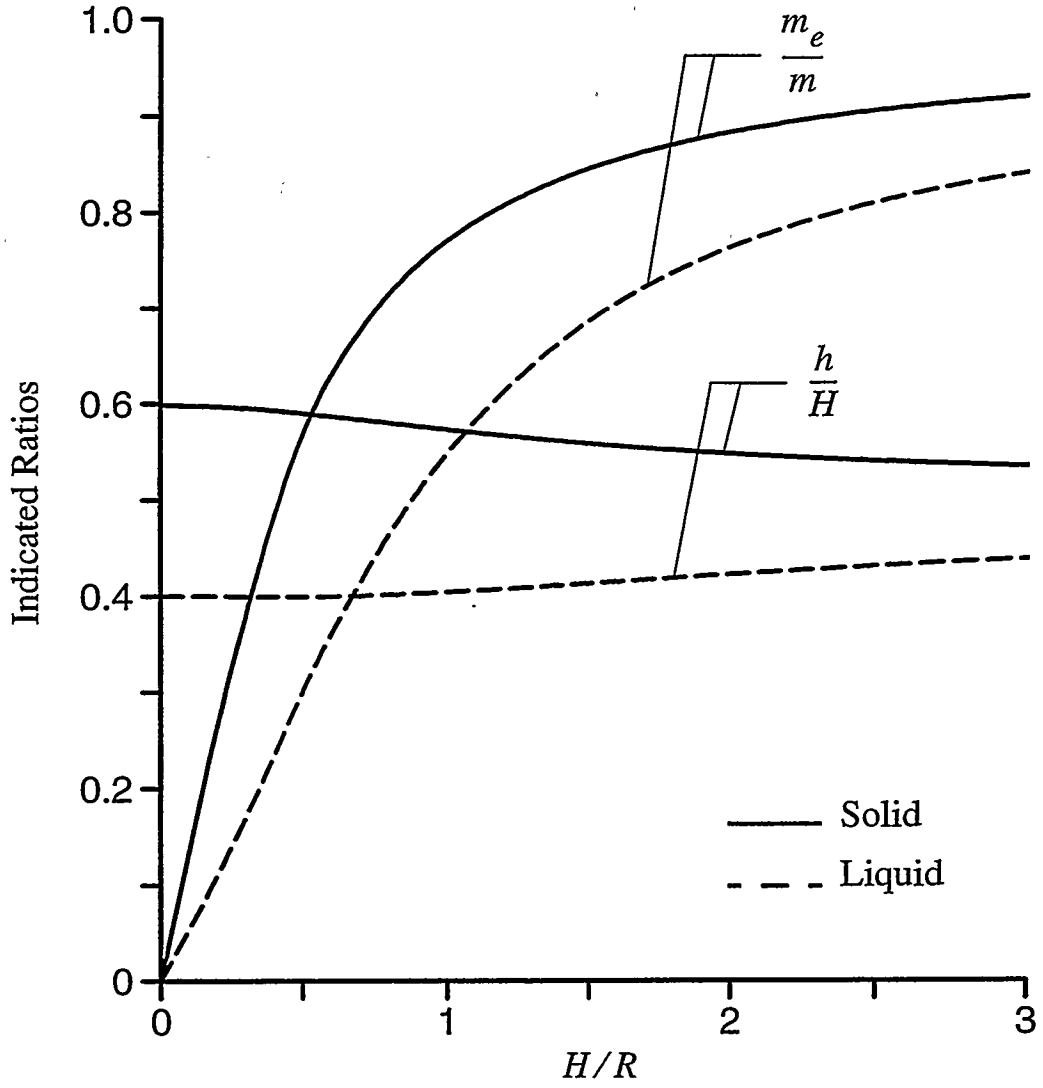

Figure 6.1 Normalized Values of Effective Mass and Effective Height for Solid- and Liquid-Containing Rigid Tanks; $m_w = 0$, solid with $\nu = 1/3$.

SECTION 7

CONCLUSIONS

Following are some of the more important conclusions of this study.

1. The relatively simple method of analysis presented is believed to define with good accuracy the effects of wall flexibility on the critical dynamic responses of horizontally excited, solid-containing cylindrical tanks. The method is expected to be particularly reliable for relatively broad systems with ratios of content-height to tank-radius of the order of unity or less.

2. By decreasing the horizontal extensional stiffness of the retained material relative to its shearing stiffness, the flexibility of the wall reduces the proportion of the inertia forces transmitted to it by extensional action and increases the proportion transmitted to the base by horizontal shearing action. The flexibility of the wall also decreases the effective damping of the retained medium, and this reduction tends to increase the amplification factor of dynamic response. With the exception of rather tall, slender systems with low to moderate wall flexibilities, for which both the shearing capacity and effective damping of the retained material are quite low, the net effect of wall flexibility is a reduction in peak response. This result is in sharp contrast with that obtained for liquid-containing tanks, for which the effect of wall flexibility is to increase rather than decrease the response.

3. For rigid tanks, the critical responses of solid-containing tanks are generally substantially larger than those of in tanks storing a liquid of the same mass density, but for flexible tanks, particularly broad tanks of high wall flexibility, the opposite is likely to be true.

4. The comprehensive numerical data presented and the analysis of these data provide not only valuable insights into the effects and relative importance of the numerous parameters involved, but also a conceptual framework for the analysis and interpretation of the solutions for more involved systems as well.

SECTION 8

REFERENCES

Rotter, J. M., and Hull, T. S. (1989). "Wall loads is squat steel silos during earthquakes." Engineering Structures, 11, 139-147.